Abstract

IWANCIO, KATHLEEN MARIE. Use of Integral Signatures and Hausdorff Distance in Planar Curve Matching. (Under the direction of Irina A. Kogan.)

Curve matching is an important problem in computer image processing and image recognition. In particular, the problem of identifying curves that are equivalent under a geometric transformation arises in a variety of applications. Two curves in $\mathbb{R}^2$ are called congruent if they are equivalent under the action of the Euclidean group, i.e. if one curve can be mapped to the other by a combination of rotations, reflections, and translations. In theory, one can identify congruent curves by using differential invariants, such as infinitesimal arc-length and curvature. The practical use of differential invariants is problematic, however, due to their high sensitivity to noise and small perturbations. Other types of invariants that are less sensitive to perturbations were proposed in literature, but are much less studied than classical differential invariants. In this thesis we provide a detailed study of matching algorithms for planar curves based on Euclidean integral invariant signatures. Several types of local and global signatures are considered. We examine numerical approximations of signatures, sensitivity to perturbation, dependence on parametrization and a choice of initial point,

and effects of the symmetries of the original image on signatures. Furthermore, we use Hausdorff distance between signatures to define a distance between congruence classes of curves.

Use of Integral Signatures and Hausdorff Distance in Planar Curve Matching

by
Kathleen Marie Iwancio

A dissertation submitted to the Graduate Faculty of
North Carolina State University
in partial fulfillment of the
requirements for the Degree of
Doctor of Philosophy

Mathematics

Raleigh, North Carolina

2009

APPROVED BY:

I. A. Kogan Chair of Advisory Committee	R. O. Fulp
P. Gremaud	K. Hollebrands

Dedication

This thesis is dedicated to my parents, Michael and Mary, who have supported me in everything I have done.

Biography

Kathleen Marie Iwancio was born November 27, 1980 in Washington, D.C. to Michael and Mary Iwancio. She has one younger brother, Matthew. Katie graduated from Elon University in 2003 with bachelors degrees in Mathematics and Physics. In August 2003 she began graduate studies in Mathematics at North Carolina State University, where she received a masters degree in December 2005. On July 18, 2009 she married Mark Lovin, who has continually supported her as she pursued her Ph.D. at North Carolina State University.

Acknowledgements

First and foremost, thanks to my advisor, Irina Kogan, for her guidance and infinite patience.

I would also like to thank members of the REU/REG group, Alex Abatzoglou, Mandy Smith, and Jessica WebsterLove for their assistance during the summer in 2007. Alex provided the main ideas of the proofs that appear in Section 3.3. Mandy and Jessica wrote a first version of the Matlab code to compute integral signatures.

Thanks to my husband Mark for his love and support. I could not have finished this thesis without him. Nor could I have finished without the love and support of my parents, Michael and Mary, to whom I have dedicated this thesis. I also thank my new family, the Lovin's, for their encouragement.

Love and thanks to my friends, especially to Laura Peveler, who has kept me smiling for the past year. Special thanks also to Michelle Snyder.

Finally, I would like to acknowledge my grandparents. Daisy and Daniel Paska taught me that I can do anything I set my mind to, and they taught me about faith. They are a large part of who I am today. I also acknowledge Carolyn Iwancio for her love. I regret that Marion Iwancio was not with us longer to lend his support.

Table of Contents

List of Tables

List of Figures

Chapter 1

Introduction

In this thesis we define distance between congruence classes of curves with respect to the Euclidean action. The motivation for this work comes from problems in computer vision, and we begin by discussing some of the approaches that are used in this field.

The general goal in machine and computer vision is to teach a computer how to "see." One of the motivations behind machine vision is the use of computers in manufacturing [68]. One of the early problems in machine vision was optical character recognition. Optical character recognition deals with reading text and converting it to machine language. This was studied as early as the 1950's [68]. Another problem in machine vision is that of pattern analysis. The study of pattern analysis has received support from several organizations, including the National Institute of Health (NIH), the military, National Aeronautics and Space Administration (NASA), and the U.S. Geological Survey (USGS).

One of the problems the NIH has been interested in is the use of pattern recognition

and analysis for use in chromosome, blood, and tissue analysis. Machine vision in general is of interest to the NIH for the purpose of understanding how the human eye works. The military, NASA, and USGS make use of surveillance photos, and have supported research and development in machine vision for the purpose of automating the interpretation of such photos [68]. As computers have become more accessible and sophisticated, the study of machine and computer vision has grown.

Some other applications in computer vision include facial recognition [21, 6, 17], document processing [7, 28, 4, 34, 11], and biomedical imaging [2, 20, 3, 56, 10, 37]. The curve matching problem has applications in automated jigsaw puzzle solving [13, 24, 67], and handwriting recognition [25]. We will briefly discuss jigsaw puzzle solving and handwriting recognition later in this chapter.

Other problems of interest include object recognition and reconstruction. The importance of invariance was recognized early in the development of computer vision [44]. One important type of invariance is that of photometric properties. The study of photometric invariance led to the development of edge detectors [44]. Another type of invariance that is important for machine and computer vision is geometric invariance. We will mention edge detection briefly and then focus on geometric invariance.

Edge Detection Edge detection is important in computer image recognition because edges form the boundary of an object, separating it from the background [49]. Many algorithms for edge detection exist. One commonly used method for edge detection is the Canny method [15]. Canny developed a method of edge detection with three specific goals. The first goal is that the edge detector should find all the edges. The second goal is to minimize the distance between the computed edge and the actual

edge. The final goal is to avoid defining multiple edges when there should be only one [15].

Some other edge detection methods include Marr-Hildreth [41], Shen-Castan [55], Roberts [51], Prewitt [50], and Sobel [58, 30]. Many other edge detection methods exist, but we will restrict our focus to Sobel edge detection. Sobel's edge detection is the method we use for our experiments in Chapter 4.

Edge detection is affected by noise and by changes in the image intensity [45]. Therefore, it is related to differentiation. The Sobel operator estimates the gradient of the brightness of the image [68]. This gradient is estimated for each image point, and shows how the image is changing, thus giving information about location and orientation of edges. The Sobel method is the default edge detection method in the Image Processing Toolbox in Matlab.

Computer Image Recognition and Geometric Invariants

One of the central problems in computer vision is computer image recognition. One wants to geometrically describe objects in images to recognize the object and to describe the object in three dimensions. There are many approaches to object recognition that rely on geometric invariants [44]. One of the difficulties in recognizing an object in an image is that the image object depends on the viewpoint. Using geometric invariants to describe the image will eliminate this problem. By using geometric invariants, one does not need to consider the position and orientation of the camera. Oftentimes image recognition is simplified to the problem of matching curves. We will discuss several methods for object recognition and curve matching.

One can use geometric invariants to create a database of images, sometimes referred to as a model library. Models in the library are often indexed by their invariant description. Use of indexing functions decreases the computation time of comparing the test image with the database.

Group Transformations The projective, affine, and Euclidean groups of transformations are most commonly used in computer vision. (For definitions, see Section 1.2.) Oftentimes the group of interest is the projective group. When obtaining an image, one projects a three-dimensional object into two-dimensions. Projective transformations consist of central projection and affine transformations. In central projection, parallel lines meet at a point. For example, consider looking at railroad tracks. As they get farther away, the tracks appear to meet. Projective transformations preserve straight lines and certain ratios to be discussed later.

On the other hand, affine transformations consist of parallel projection and similarity transformations. Affine transformations also preserve lines, and parallel lines do not appear to meet.

Another group of interest in computer vision is the Euclidean group, consisting of reflections, rotations, and translations. In applications such as jigsaw puzzle assembly, the special Euclidean group is of interest.

Compared to the groups mentioned thus far, the projective group is the most general. The invariants for the projective group action are the most complex because the transformations have more parameters than Euclidean, similarity, or affine transformations.

Algebraic Invariants One class of invariants that can be used in image recognition is the class of algebraic invariants. In [52], Rothwell et al., consider matching images against a database of known objects. They use algebraic invariants to find shape descriptions that index the library. Using indexing functions prevents one from having to test the image against every model in the library. Rothwell et al. fit an algebraic curve to a set of points and compute several projective invariants to define a "feature vector." The feature vector gives a hypothesized match. The match is then tested by transforming the model in the database to the image.

To compute algebraic invariants, one estimates a curve by a polynomial. In [62], Weiss points out a couple of problems with algebraic invariants.

1. It is not always possible to find a polynomial fit for a shape.

2. Algebraic invariants are global and not equipped to deal with occlusions.

Joint invariants are also used in computer vision. Joint invariants depend on sets of points, lines, conics, etc. extracted from the image. In [18], Coehlo et al. discuss the use of several projective joint invariants in computer vision applications. For example, let l_1 and l_2 represent two lines, and let x_1 and x_2 be two points. Let $l_i x_j$ represent the distance between line l_i and point x_j. Then $I_1 = \frac{l_1 x_1}{l_2 x_1} \cdot \frac{l_2 x_2}{l_1 x_2}$ is a joint invariant under the action of the projective group.

Another joint invariant under the projective action that is discussed in [18] is defined by considering the coefficient matrices for two coplanar conic curves, C_1 and C_2. The conics are defined by $\mathbf{x}^t C_i \mathbf{x} = 0$, where $\mathbf{x}^t = (x, y, z)$. Then $I_1 = trace(C_1^{-1} C_2)$ and $I_2 = trace(C_2^{-1} C_1)$ are projective invariants.

In [48], Olver classifies joint invariants, depending on sets of points extracted from the image, under the actions of the Euclidean, equi-affine, affine, and projective groups.

The Euclidean distance between two points is a joint invariant under the action of the Euclidean group. The interpoint Euclidean distances generate all joint invariants for the Euclidean group action.

Suppose we have a simplex with vertices $\mathbf{x}_1, \ldots, \mathbf{x}_{m+1}$ in $\mathbb{R}^m$, where $\mathbf{x}_i = (x_i^1, \ldots x_i^m)^t$. Then the signed volume of this simplex is defined by

$$V(1, 2, \ldots m+1) = \frac{(-1)^m}{m} det \begin{pmatrix} \mathbf{x}_1 & \mathbf{x}_2 & \ldots & \mathbf{x}_{m+1} \\ 1 & 1 & \ldots & 1 \end{pmatrix}. \tag{1.1}$$

All joint invariants for the special affine group action are functions of such volumes. The joint invariants for the affine group, $A(m)$, acting on $\mathbb{R}^m$ are generated by ratios of simplex volumes.

Now consider the action of the projective group, $PSL(m+1, \mathbb{R})$ on $\mathbb{R}^m$. All joint invariants are functions of the cross-ratio of volumes (1.1). For the one-dimensional case, the cross ratio is defined by:

$$\frac{(x_2 - x_1)(x_4 - x_3)}{(x_2 - x_3)(x_4 - x_1)}.$$

If we consider the action of $PSL(2, \mathbb{R})$, then the joint invariants of five points are generated by two cross-ratios. These cross-ratios are defined by:

$$\frac{V(1,2,3)V(1,4,5)}{V(1,2,4)V(1,3,5)}, \quad \frac{V(1,2,3)V(2,4,5)}{V(1,2,4)V(2,3,5)}.$$

Notice that $V(1,2,3) = \frac{1}{2} det \begin{pmatrix} x_1^1 & x_2^1 & x_3^1 \\ x_1^2 & x_2^2 & x_3^2 \\ 1 & 1 & 1 \end{pmatrix}$, and the other volumes are computed similarly.

Some examples of applications of joint invariants for points can be found in [35, 9, 31, 42].

Moment Invariants In [32], Hu introduces the use of moment invariants in pattern recognition. In [59], Taubin and Cooper present a method for matching planar curves under the action of the affine group. Their method can be used to recognize objects in cluttered environments. The authors use moment invariants to index images for comparison against a database.

Taubin and Cooper compute moment invariants given a grey scale image represented by a function f. A moment is an integral of the form

$$\int_{\mathbb{R}^2} g(x,y) f(x,y) dx dy,$$

where g is a polynomial in variables x and y [19]. It is sufficient to choose a monomial function $g(x,y) = x^i y^j$. One can take translation into consideration by considering normalized moments. Normalized moments are computed by translating the image so that its center of mass is located at the coordinate origin [19]. One then considers how the moments are affected by linear transformations. Taubin and Cooper compute affine moment invariants as functions of normalized invariants by reducing the problem to one of computing eigenvalues for square matrices [59].

Xu and Li also apply affine moment invariants to 3-dimensional object recognition in [65]. Applications of moment invariants in image analysis are also discussed in [43].

Differential Invariants and Signatures A possible solution to the problems presented by algebraic invariants, is to consider differential invariants. Differential invariants may be used for local comparison, and thus are well-equipped for images with occlusions. Euclidean curvature and the derivative of curvature with respect to arc length are two well known differential invariants. One can similarly define differential invariants for the affine and projective group actions. The difficulty is that the curvatures for different parametrizations of a curve may not coincide. A curve can always be reparametrized with respect to arc length, but this may be very difficult in practice. In [5], and [14], the authors use differential invariants for the Euclidean, affine, and projective group actions to define differential signatures. Differential signatures may be used to solve the curve matching problem, and they have the advantage of being independent of a choice of parameter. The practical utilization of differential signatures is problematic due to the sensitivity of derivatives to small perturbations.

Weiss considers affine and projective differential signatures, based on arc length and curvatures, and presents more robust methods for computation of differential invariants [62]. One of the computational difficulties is that the curve of interest is given by a parametrization $(x(t), y(t))$, with t being some arbitrary and not necessarily invariant parameter. Weiss remarks that the necessary order of differentiation can be reduced if the parameter problem is eliminated. In [62], Weiss presents a method that does not have the problem of parametrization, thus reducing the order of differentiation needed. By reducing the order of differentiation needed to compute differential invariants, the

effects of noise and small perturbations are reduced. Weiss' method relies on a change of coordinates, such that some of the derivatives are already defined. He calls the new coordinate system a "canonical" system.

Semi-Differential Invariants Van Gool et al. consider semi-differential invariants in [60]. Their discussion is limited to planar contours. The method presented is a combination of correspondence searching and numerical differentiation. In a correspondence search, one looks for corresponding points on a contour in the image and a model contour. Van Gool et al. use reference points when prolonging the action of the group to derivatives. The use of reference points and differentiation is what leads to these semi-differential invariants. The authors look for invariants of a predefined form to avoid having to solve systems of partial differential equations. By predefining the form of the invariant, they reduce the problem to solving a system of linear equations. The drawback is that this approach will only find invariants of the predefined form and does not necessarily compute a complete set of invariants.

Brill et al. consider invariants that may also be classified as semi-differential [12]. The authors compute derivatives along a curve, but they use multiple image points to reduce the order of differentiation that is necessary for computing differential invariants. These invariants are based on the tangents of a curve, curvature, and torsion.

We emphasize that the use of semi-differential invariants decreases the effects of noise and small perturbations because the necessary order of differentiation is reduced. Another approach to reducing the effects of noise and small perturbations is the use of integro-differential invariants as discussed in [53]. Sato and Cipolla consider the actions of the Euclidean and Affine groups on curves. They define invariants that are

integrals of the Euclidean and affine curvatures.

Integral Invariants The use of strictly integral invariants will further reduce the effects of noise and small perturbations. Hann and Hickman define potentials and use them to calculate integral invariants for the Euclidean and affine group actions on curves in $\mathbb{R}^2$ [29]. There are challenges defining such invariants for the projective group action on curves in $\mathbb{R}^2$, so the authors use integro-differential invariants in this case.

Manay et al. introduce two integral invariants with respect to the Euclidean and similarity groups [40]. These invariants are based on distance and area. The integral invariant based on area will be discussed further in Chapter 4 in this thesis. They plot a signature curve parametrized by the derivative of the integral area invariant and the integral area invariant. This signature depends on the choice of initial point. They also briefly mention using the Hausdorff distance between signature curves as a way of defining the distance between shapes. However, they do not run experiments based on this definition of distance.

In [23], Feng, Kogan, and Krim define potentials as in [29] and use inductive variation, [36], of the moving frame method, [46], to calculate strictly integral invariants for the Euclidean and affine actions on curves in $\mathbb{R}^2$ and $\mathbb{R}^3$. As in the case of differential invariants, the integral invariants depend on the choice of parameter. To avoid this dependence, the authors define an integral signature. Two types of signatures are defined in [23], a global signature that involves integration along the entire curve, and a local signature that involves integration on segments of the curve.

Applications of Euclidean Curve Matching As this thesis concentrates on the problem of equivalence for planar curves under Euclidean group actions, we would like to specifically mention two of many possible applications of Euclidean curve matching.

Jigsaw Puzzle Application One of the applications of curve matching with respect to the Euclidean group is the automated solution of an apictorial jigsaw puzzle, which arises, in particular, in programming assembly robots. Assembly depends only on the shape of the puzzle pieces. We discuss one of many methods for jigsaw puzzle solving.

In [64], Wolfson uses a method for curve matching that is similar to the method presented in [14]. Wolfson et al. discuss the use of curve matching for automated jigsaw puzzle matching in [63].

Oftentimes, one begins solving a jigsaw puzzle by identifying "frame" pieces vs. "interior" pieces. The frame pieces will have at least one straight edge. Examples of this type of approach can be found in [13, 24, 67]. For example, to assemble a jigsaw puzzle, Zisserman et al. [67] assume that each piece consists of four sides. The sides are classified as edges, tabs, or slots based on concavity. Their matching algorithm begins placing a corner, which has two straight edges. This corner piece defines a frame for the puzzles construction. The puzzle is then assembled piece by piece based on the fact that the tabs and slots will have the same invariant shape description.

Handwriting Recognition Liu et al. discuss past methods for handwriting recognition and present new methods in [38]. Smirnova and Watt have developed a user interface called Mathink that can be used on Tablet PCs, and SmartBoards. They

discuss Mathink and mathematical handwriting recognition in [57].

In [25], Golubitsky et al. consider the use of the integral invariants computed in [23] for recognizing handwritten characters independent of their orientation. The trace of the symbol is a two-dimensional curve, so symbol recognition is a problem of classifying curves. Golubitsky et al. consider a method of classifying curves based on integral invariants and compare it to a method based on geometric moment functions. They focus on the action of the special orthogonal group, i.e. the group of rotations.

The authors conclude that using integral invariants to classify curves performs better than the method using moment invariants. In addition, the use of integral invariants is more efficient computationally [25].

Thesis Outline The goal of this thesis is to complete a detailed study of Euclidean integral invariants and integral signatures for curves in $\mathbb{R}^2$. In particular, we study global and local Euclidean signatures. In addition, we study the use of Hausdorff distance to define the distance between congruence classes of curves. We occasionally restrict our interest to classifying curves under the action of the special Euclidean group.

This thesis begins with a statement of the curve matching problem and provides background material on group actions, prolongations of group actions, and various types of invariants. A brief discussion of the use of differential invariants for curve matching follows. As previously mentioned, the use of differential invariants is problematic due to their sensitivity to small perturbations, so we follow the work of [29] and [23] to define integral invariants and signatures.

We study the properties of integral signatures and their numerical approximations,

making some observations on how symmetries of the original curve are reflected in the signature. We then define distance between congruence classes of curves as the Hausdorff distance between signatures. The advantage to using Hausdorff distance is that it is independent of parametrization and starting point. We conclude our thesis with experiments and a comparison of our methods with the method presented in [39].

Siddharth Manay et al. calculate use an area integral invariant, and define a distance between equivalence classes of curves, which they call a group invariant distance. This group invariant distance is a modification of the L^2 distance between integral invariants as functions of arc length. Manay et al. define distance between shapes as the invariant distance between boundaries. Thus the distance between shapes has the following desirable properties, 1) the distance is zero if the shapes are equivalent under Euclidean transformations, and 2) the distance is small if there is a small perturbation of the image. Note that our goal is also to define distance between congruence classes so that these properties hold. The authors of [39] test their results on some images from the Kimia silhouette database found at http://www.lems.brown.edu/vision/software/index. We also use the Kimia silhouette database to test our algorithms for curve matching.

1.1 Curve Matching Problem

Given a group action on a manifold, two submanifolds are equivalent if one can be mapped to the other by an element of the group. In general, given a group action, one may be interested in finding classes of equivalent manifolds and describing the

symmetry groups of each class of manifolds.

In this thesis we are particularly interested in the equivalence problem for curves in $\mathbb{R}^2$ under the action of the Euclidean group and therefore give the following definition.

Definition 1.1.1. *Two curves in $\mathbb{R}^2$ are* **congruent** *if there is an element of the Euclidean group that maps one curve to the other.*

We work with parametric curves $\gamma(t) = \{(x(t), y(t)) | t \in I_\gamma\} \subseteq \mathbb{R}^2$, where I_γ is an interval in $\mathbb{R}$. Congruence of γ_1 and γ_2 is denoted by $\gamma_1 \cong \gamma_2$, and $[\gamma_1]$ denotes the class of curves congruent to γ_1.

1.2 Group Actions

We begin by reviewing some basic facts about group actions. For a more detailed presentation, see [8].

Definition 1.2.1. *Let G be a group and let S be a set. The action of G on S is a mapping $\alpha : G \times S \to S$ satisfying the following:*

1. *$\alpha(e, s) = s$, where e is the identity in G and s is any element in S.*
2. *$\alpha(gg', s) = \alpha(g, \alpha(g', s))$ for all $g, g' \in G$ and $s \in S$.*

We will usually denote the action by $\alpha(g, s) = gs$.

An example of a group action is the action of the general linear group, $GL(n)$ on $\mathbb{R}^n$. One can also consider several important subgroups of $GL(n)$. One such subgroup is the special linear group, $SL(n)$, defined as the set $\{A \in GL(n) | det(A) = 1\}$. Two

other important subgroups are the orthogonal group, $O(n)$, and the special orthogonal group $SO(n)$. The orthogonal group is defined as $O(n) = \{A \in GL(n) | A^T A = I\}$. The special orthogonal group is defined by $SO(n) = \{A \in O(n) | det(A) = 1\}$.

Notice that $O(2)$ is the set of rotations and reflections on the plane, and $SO(2)$ is the set of rotations on the plane. Some other examples are the actions of the Euclidean, affine, similarity, and projective groups. We denote the Euclidean group acting on $\mathbb{R}^n$ by $E(n)$ and the affine group by $A(n)$. These groups are defined as the semi-direct products of matrix groups with $\mathbb{R}^n$.

$$\begin{aligned} E(n) &= O(n) \ltimes \mathbb{R}^n \\ A(n) &= GL(n) \ltimes \mathbb{R}^n. \end{aligned}$$

The similarity group is defined as the direct product $\mathbb{R} \times E(n)$. Another group which plays an important role in computer vision is the projective group, $PSL(n+1, \mathbb{R})$. The projective group is defined as the quotient $GL(n+1, \mathbb{R})/\{\lambda I\}$, where λ is a nonzero real number, and I is a unit matrix.

Example 1.2.2 (Projective Group Action on $\mathbb{R}^2$)**.** *The local action of* $PSL(3, \mathbb{R})$ *on* $\mathbb{R}^2$ *is given by:*

$$\begin{aligned} \bar{x} &= \frac{a_{11}x + a_{12}y + a_{13}}{a_{31}x + a_{32}y + a_{33}} \qquad (1.2) \\ \bar{y} &= \frac{a_{21}x + a_{22}y + a_{23}}{a_{31}x + a_{32}y + a_{33}}. \end{aligned}$$

The above action is defined for $a_{31}x + a_{32}y + a_{33} \neq 0$.

Note that $\mathbb{R}^2$ *can be embedded in* $\mathbb{P}^2$. *In homogeneous coordinates, the point* (x, y) *in* $\mathbb{R}^2$ *corresponds to the point* $(x, y, 1)$ *in* $\mathbb{P}^2$.

Let $A \in GL(3, \mathbb{R})$ *be given by*

$$A = \begin{pmatrix} a_{11} & a_{12} & a_{13} \\ a_{21} & a_{22} & a_{23} \\ a_{31} & a_{32} & a_{33} \end{pmatrix}.$$

In homogeneous coordinates the action 1.2 corresponds to:

$$\begin{pmatrix} \bar{x} \\ \bar{y} \\ \bar{z} \end{pmatrix} = \begin{pmatrix} a_{11} & a_{12} & a_{13} \\ a_{21} & a_{22} & a_{23} \\ a_{31} & a_{32} & a_{33} \end{pmatrix} \begin{pmatrix} x \\ y \\ 1 \end{pmatrix}.$$

Example 1.2.3 (Affine Group Action on $\mathbb{R}^2$)**.** *The affine group,* $A(2, \mathbb{R})$ *acts on* $\mathbb{R}^2$ *in the following way:*

$$\begin{aligned} \bar{x} &= a_{11}x + a_{12}y + v_1 \\ \bar{y} &= a_{21}x + a_{22}y + v_2, \end{aligned}$$

where $a_{11}, a_{12}, a_{21}, a_{22}, v_1, v_2$ *are real numbers.*

The affine group is a subgroup of the projective group. We can represent (x, y) *as*

a column vector $\mathbf{x} = (x, y, 1)^t$*, and the action of* $A(2, \mathbb{R})$ *can be written as the product:*

$$\begin{pmatrix} \bar{x} \\ \bar{y} \\ 1 \end{pmatrix} = \begin{pmatrix} a_{11} & a_{12} & v_1 \\ a_{21} & a_{22} & v_2 \\ 0 & 0 & 1 \end{pmatrix} \begin{pmatrix} x \\ y \\ 1 \end{pmatrix} = \begin{pmatrix} a_{11}x + a_{12}y + v_1 \\ a_{21}x + a_{22}y + v_2 \\ 1 \end{pmatrix}.$$

Example 1.2.4 (Euclidean Group Action on $\mathbb{R}^2$)**.** *The Euclidean group action consists of reflections, rotations, and translations. The transformations are given by:*

$$\begin{aligned} \bar{x} &= \cos\phi\, x - \epsilon \sin\phi\, y + v_1 \\ \bar{y} &= \sin\phi\, x + \epsilon \cos\phi\, y + v_2, \end{aligned}$$

where $v_1, v_2, \phi \in \mathbb{R}$ *and* $\epsilon = \pm 1$*.*

Notice that the Euclidean group is a subgroup of the affine group. Thus, the action of the Euclidean group can be written similarly as:

$$\begin{pmatrix} \bar{x} \\ \bar{y} \\ 1 \end{pmatrix} = \begin{pmatrix} \cos\theta & -\epsilon\sin\theta & v_1 \\ \sin\theta & \epsilon\cos\theta & v_2 \\ 0 & 0 & 1 \end{pmatrix} \begin{pmatrix} x \\ y \\ 1 \end{pmatrix} = \begin{pmatrix} \cos\theta\, x - \epsilon\sin\theta\, y + v_1 \\ \sin\theta\, x + \epsilon\cos\theta\, y + v_2 \\ 1 \end{pmatrix}.$$

We will focus primarily on the action of the special Euclidean group, $SE(2)$, which is defined as above, with $\epsilon = 1$.

Example 1.2.5 (Similarity Group Action on $\mathbb{R}^2$)**.** *The similarity group is also a sub-*

group of the affine group, with action on $\mathbb{R}^2$ *given by:*

$$\begin{aligned} \bar{x} &= \lambda(\cos\phi\, x - \sin\phi\, y) + v_1 \\ \bar{y} &= \lambda(\sin\phi\, x + \cos\phi\, y) + v_2, \end{aligned}$$

for $v_1, v_2 \in \mathbb{R}$ *and a nonzero real number,* λ*.*

The action of the similarity group on $\mathbb{R}^2$ *can also be written as the matrix product:*

$$\begin{pmatrix} \bar{x} \\ \bar{y} \\ 1 \end{pmatrix} = \begin{pmatrix} \lambda\cos\phi & -\lambda\sin\phi & v_1 \\ \lambda\sin\phi & \lambda\cos\phi & v_2 \\ 0 & 0 & 1 \end{pmatrix} \begin{pmatrix} x \\ y \\ 1 \end{pmatrix}.$$

where λ *is a real number not equal to zero. This group consists of reflections, rotations, scaling, and translations.*

Definition 1.2.6. *Let* $s \in S$*. The* **orbit** *of* s *is defined as the set of points* $orb_G(s) = \{gs \in S | g \in G\}$*.*

The orbits of two points are either equal or disjoint. As a result, orbits provide a partition of the set S into equivalence classes.

Example 1.2.7. *Consider the group of rotations,* $SO(2)$*, acting on the plane. The orbit of the origin is the origin. The orbit of any other point in the plane is a circle. See Figure 1.1.*

Example 1.2.8. *The orbit for any point* $(x, y) \in \mathbb{R}^2$ *under the Euclidean group action is* $\mathbb{R}^2$*.*

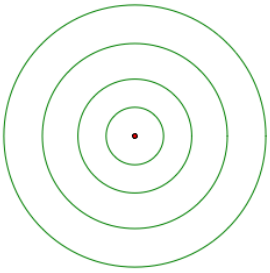

Figure 1.1: Orbits for $SO(2)$ acting on the plane

Example 1.2.9. *Similarly, the orbit for $(x, y) \in \mathbb{R}^2$ under the affine group action is the entire plane.*

Definition 1.2.10. *The action of G on S is said to be* **transitive** *if there exists an $s \in S$ such that $orb_G(s) = S$.*

We can show that if the action is transitive, then $orb_G(s) = S$ for every $s \in S$.

Proof. Suppose G is a group acting transitively on S. Let $s' \in S$ be an element such that $orb_G(s') = S$. Consider another point $s_1 \in S$. We know $s_1 \in orb_G(s_1)$ because $es_1 = s_1$. Hence $orb_G(s_1) \neq \{\emptyset\}$. Suppose $orb_G(s_1) \neq S$. Then $orb_G(s_1) \cap orb_G(s') = \{\emptyset\}$ because orbits are equal or disjoint. This implies that $orb_G(s_1) = \{\emptyset\}$ which is a contradiction. Therefore $orb_G(s_1) = S$. □

Definition 1.2.11. *The* **stabilizer** *of a point $s \in S$ is the set $G_s = \{g \in G | gs = s\}$.*

It is a simple exercise to prove that the stabilizer forms a subgroup, often referred to as the **isotropy group**.

Example 1.2.12. *Let G be $SO(2)$ and let S be the plane. Suppose s is a point other than the origin. Then the stabilizer of s is the subgroup containing the identity of*

$SO(2)$ and rotations by integer multiples of 2π. The isotropy group of the origin is the entire group.

Definition 1.2.13. *The action of G on S is called* **free** *if $G_s = \{e\}$ for all $s \in S$.*

In other words, the action is free if the identity element is the only element that stabilizes all points in S.

Definition 1.2.14. *Let $H = \bigcap_{s \in S} G_s$. The set H is called the* **global stabilizer**. *The action of G on S is called* **effective** *or* **faithful** *if $H = \{e\}$.*

One can easily show that the global stabilizer is a normal subgroup. The global stabilizer may also be referred to as the **global isotropy group**.

The group action is effective if each group element acts differently on the set. This is equivalent to saying that the identity element of the group is the only identity transformation acting on the set [46].

1.3 Invariants

Definition 1.3.1. *For G acting on S, a function $f : S \to \mathbb{R}$ is an* **invariant** *if $f(gs) = f(s)$ for all $g \in G$ and $s \in S$.*

It is worth noting that any function of an invariant is also an invariant. Also, invariant functions are constant along the orbits. Depending on a class of actions, different types of invariants may be considered. For example, if α is the action of an algebraic group on an algebraic variety, then we would be interested in finding polynomial and/or rational invariants [61].

Example 1.3.2. *Consider the action of* $\mathbb{R}$ *on* $\mathbb{R}^2$ *given by* $(x, y) \mapsto (x + \epsilon, y)$ *for a real number* ϵ*. The orbit of a point* (x, y) *is a horizontal line passing through this point. Then a generating invariant for this action is given by* $I(x, y) = y$*. In other words, any function of* y *is an invariant for this group action. This is a simple example of a polynomial invariant.*

Example 1.3.3. *Consider the action of* $\mathbb{R}$ *on* $\mathbb{R}^2$ *given by* $(x, y) \mapsto (e^\epsilon x, e^\epsilon y)$*, where* $\epsilon \in \mathbb{R}$*. The orbits are open rays through the origin. Then a rational invariant for this action is given by* $f(x, y) = \frac{x}{y}$*. Notice that* f *is not defined for all of* $\mathbb{R}^2$ *because it is undefined for* $y = 0$*. There are no polynomial invariants for this action.*

In this thesis, we consider the actions of Lie groups on smooth manifolds and are interested in finding smooth or locally smooth invariants. We begin with the definition of local and global invariants for Lie groups acting on smooth manifolds.

Definition 1.3.4. *Suppose* G *is a Lie group acting on a smooth manifold,* M*. Let* $\mathcal{U}$ *be an open subset of* M*. A function* $f : M \to \mathbb{R}$ *defined on* $\mathcal{U}$ *is a* **local invariant** *if* $f(gx) = f(x)$ *for every* $x \in \mathcal{U}$ *and every* g *in some neighborhood* $\mathcal{V} \subset G$*, where* $\mathcal{V}$ *contains the group identity and may or may not depend on* x*. The function* f *is* **globally invariant** *if* $f(gx) = f(x)$ *for all* $x \in \mathcal{U}$ *and for all* $g \in G$ *such that* $gx \in \mathcal{U}$ *[46].*

Definition 1.3.5. *For a Lie group* G *acting on a smooth manifold* M*, an invariant function* $f : M \to \mathbb{R}$ *is* **locally smooth** *if it is infinitely differentiable on some neighborhood of* M*. The function* f *is smooth if it is infinitely differentiable on* M*.*

Example 1.3.6. *If we look again at $SO(2)$ acting on the points in the plane, then the function $r(x,y) = \sqrt{x^2+y^2}$ is a global invariant. The invariant function r is simply the distance from the origin to a point (x,y). The function r is locally smooth. Notice that because $\frac{\partial r}{\partial x} = \frac{x}{\sqrt{x^2+y^2}}$, the function is not smooth in a neighborhood of $(x,y) = (0,0)$.*

One could also consider the invariant $r_1 = x^2 + y^2$, which is a polynomial invariant for $SO(2)$ acting on points in the plane. This is a smooth global invariant. In some situations, it may be advantageous to consider a polynomial invariant.

Example 1.3.7. *Consider the action $\alpha : G \times \mathbb{R}^2 \to \mathbb{R}^2$, where $G = \{(\epsilon,\tau)|\epsilon \in \mathbb{R}, \tau = \pm 1\}$ acts on a point (x,y) by $(x+\epsilon, \tau y)$. The orbit of a point (x,y), where $y \neq 0$, consists of a horizontal line passing through (x,y) and a horizontal line passing through $(x,-y)$. The orbit of a point $(x,0)$ is the x-axis. Then a generating invariant for α is $I(x,y) = y^2$. Notice that $f(x,y) = y$ is a local invariant, since f is an invariant for the subgroup of G, consisting of elements $g \in \{(\epsilon,1)|\epsilon \in \mathbb{R}\}$.*

There is an algorithm for finding a generating set of local smooth invariants called the cross-section, or moving frame method. This method is based on the work of Cartan, Griffiths, Green, Fels, and Olver [16, 27, 26, 22]. Any other local smooth invariant is a smooth function of generating invariants.

Chapter 2

Differential Signature

2.1 Differential Invariants

We will now consider the action of the special Euclidean group, $SE(2,\mathbb{R})$ on the plane, $\mathbb{R}^2$. In other words, we consider rotations and translations of points in the plane. This action is transitive, so the only invariants are constants. However, the induced action on the infinite dimensional space of curves is not transitive and will produce non-constant invariants. Let γ be a curve parametrized by $(x(t), y(t))$ for t in some interval $I_\gamma \subset \mathbb{R}$. Then the action on γ is given by:

$$\begin{aligned} \bar{x}(t) &= \cos(\phi)x(t) - \sin(\phi)y(t) + a \\ \bar{y}(t) &= \sin(\phi)x(t) + \cos(\phi)y(t) + b. \end{aligned} \tag{2.1}$$

We prolong the action of $SE(2,\mathbb{R})$ to the curve and its derivatives. Using the chain

rule:

$$\begin{aligned}
\frac{d\bar{y}}{d\bar{x}}(t) &= \frac{\frac{d\bar{y}}{dt}}{\frac{d\bar{x}}{dt}} = \frac{\sin\phi\dot{x}(t) + \cos\phi\dot{y}(t)}{\cos\phi\dot{x}(t) - \sin\phi\dot{y}(t)} \\
\frac{d^2\bar{y}}{d\bar{x}^2} &= \frac{\frac{d}{dt}\left(\frac{d\bar{y}}{d\bar{x}}\right)}{\frac{d\bar{x}}{dt}} = \frac{\dot{x}(t)\ddot{y}(t) - \ddot{x}(t)\dot{y}(t)}{(\cos\phi\dot{x}(t) - \sin\phi\dot{y}(t))^3} \qquad (2.2) \\
\frac{d^3\bar{y}}{d\bar{x}^3}(t) &= \frac{\frac{d}{dt}\left(\frac{d^2\bar{y}}{d\bar{x}^2}\right)}{\frac{d\bar{x}}{dt}} \\
&= \frac{(\cos\phi\dot{x}(t) - \sin\phi\dot{y}(t))(\dot{x}(t)\dddot{y}(t) - \dddot{x}(t)\dot{y}(t)) - 3(\dot{x}(t)\ddot{y}(t) - \ddot{x}(t)\dot{y}(t)}{(\cos\phi\dot{x}(t) - \sin\phi\dot{y}(t))^5} \\
&\vdots
\end{aligned}$$

The dots denote differentiation with respect to t.

Definition 2.1.1. *A* **differential invariant** *is an invariant function under the prolonged action given in equations (2.1) and (2.2).*

Then two well known differential invariants for this action are the Euclidean curvature and the derivative of curvature with respect to arc length. The invariant differential form $ds = \sqrt{\dot{x}^2(t) + \dot{y}^2(t)}dt$ gives us the arc length parameter $s = \int_{t_0}^{t} ds$. We can then define the invariant differential operator $\frac{d}{ds} = \frac{1}{\sqrt{\dot{x}^2(t)+\dot{y}^2(t)}}\frac{d}{dt}$. Using this invariant differential operator, we can write curvature and its derivative with respect to arc length:

$$\begin{aligned}\kappa(t) &= \frac{\dot{x}(t)\ddot{y}(t) - \ddot{x}(t)\dot{y}(t)}{(\dot{x}^2(t) + \dot{y}^2(t))^{\frac{3}{2}}} \\ \kappa_s(t) &= \frac{d}{ds}\kappa(t) = \frac{1}{\sqrt{\dot{x}^2(t) + \dot{y}^2(t)}}\frac{d}{dt}\kappa(t) \\ &= \frac{(\dot{x}^2 + \dot{y}^2)(\dot{x}\dddot{y} - \dddot{x}\dot{y}) - 3(\dot{x}\ddot{x} + \dot{y}\ddot{y})(\dot{x}\ddot{y} - \ddot{x}\dot{y})}{(\dot{x}^2 + \dot{y}^2)^3}.\end{aligned} \tag{2.3}$$

The curvature and its derivative are invariants under transformations that are sufficiently close to the identity of the group. If we were to rotate by π, the signs would change. To make these global invariants, we instead use the absolute values, $|\kappa(t)|$ and $|\kappa_s(t)|$. By taking absolute value, we obtain invariants for the entire Euclidean group action. Restated, $|\kappa(t)|$ and $|\kappa_s(t)|$ are invariant with respect to rotations, translations, and reflections.

In the next section, we will look at the use of curvature and its derivative for classifying curves.

2.2 Differential Signature

We want to determine whether one curve can be transformed to another by a rigid motion. It is known that if two curves have the same curvature as a function of arc length, then they are equivalent under rigid motion. In practice, it is often difficult to reparametrize the curve based on arc length. Under an arbitrary parametrization, the curvatures of equivalent curves may not match. Consider the following example.

Example 2.2.1. *Consider the following curve under different parametrizations,* $\gamma =$

$(t, \cos t)$ *and* $\tilde{\gamma} = (t^3, \cos t^3)$*, where* $t \in [0, \pi]$*. These parametrizations determine the same curve, but the curvatures look very different. See Figure 2.1. In the figure,* t *is on the horizontal axis, and* $\kappa(t)$ *is on the vertical axis.*

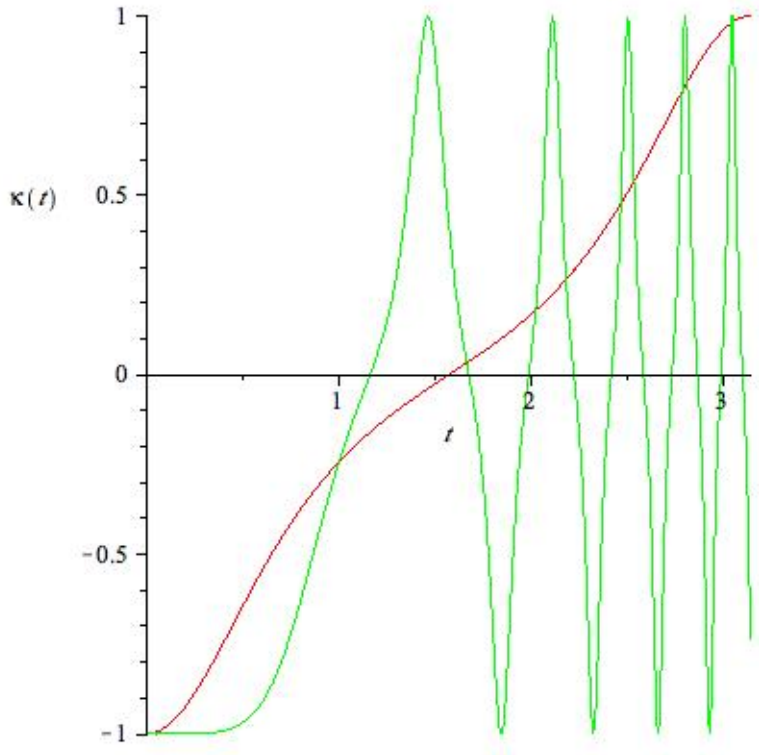

Figure 2.1: Graph of κ as a function of t for $\gamma = (t, \cos t)$ and $\tilde{\gamma} = (t^3, \cos t^3)$

We instead consider the differential Euclidean signature curve parametrized by $(|\kappa(t)|, |\kappa_s(t)|)$, where $\kappa(t)$ is the Euclidean curvature and $\kappa_s(t)$ is the derivative of curvature with respect to arc length. The advantage to using the differential Euclidean signature is that it does not depend on the parametrization [14]. We give a precise definition of signature curve in Chapter 3.

Theorem 2.2.2. *If the differential Euclidean signature curves for two C^3 smooth curves overlap, then local segments of the two C^3 smooth curves can be mapped to each other by a combination of rotations, translations, and reflections.*

For a proof of Theorem 2.2.2, see [14] or [47].

Again, consider $\gamma = (t, \cos(t))$ and $\tilde{\gamma} = (t^3, \cos(t^3))$, for $t \in [0, \pi]$. The differential Euclidean signature for both parametrizations is given in Figure 2.2.

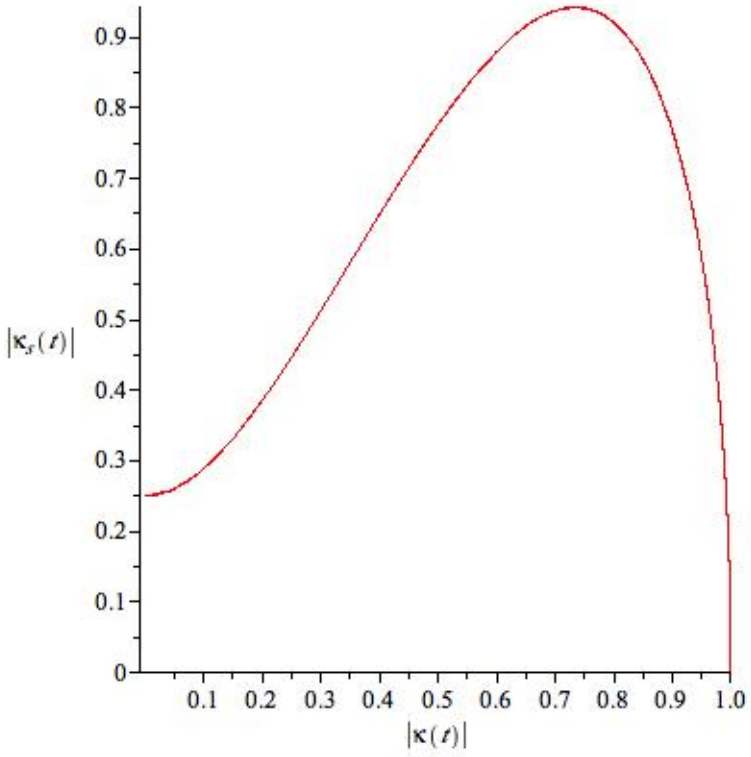

Figure 2.2: Euclidean differential signature, $(|\kappa|, |\kappa_s|)$ for $\gamma = (t, \cos t)$ and $\tilde{\gamma} = (t^3, \cos t^3)$

The Euclidean differential signatures for the different parametrizations coincide as expected. Again we will consider the curve $\gamma = (t, \cos t)$ for $t \in [0, \pi]$. A rotation of γ

by 45° is given by $\overline{\gamma} = (\frac{\sqrt{2}}{2}t - \frac{\sqrt{2}}{2}\cos t, \frac{\sqrt{2}}{2}t + \frac{\sqrt{2}}{2}\cos t)$.

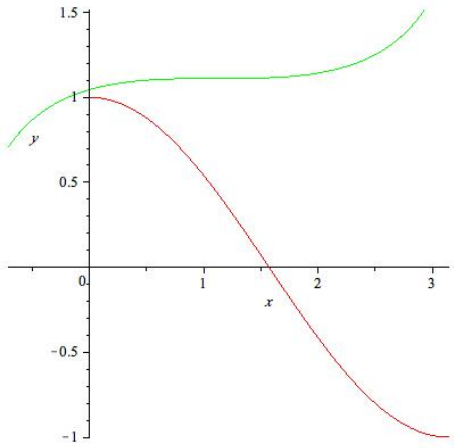

Figure 2.3: Graph of $\gamma = (t, \cos t)$ and a 45° rotation of γ

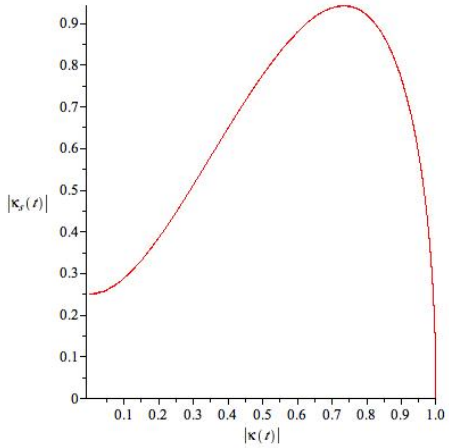

Figure 2.4: Euclidean differential signature, $(|\kappa|, |\kappa_s|)$ for $\gamma = (t, \cos t)$ and a 45° rotation of γ

We observe in Figure 2.4 that the differential signatures for these curves do in fact coincide. Now we consider a small perturbation of the cosine curve defined in equation (2.5).

Example 2.2.3. *Consider the curves defined by*

$$\gamma(t) = (t, \cos(t)), \tag{2.4}$$

$$\tilde{\gamma}(t) = = (t + \frac{1}{100}\cos(100t), \cos(t) + \frac{1}{100}\sin(100t)) \tag{2.5}$$

for $t \in [0, \pi]$.

The curve $\tilde{\gamma}$ is a small perturbation of γ. The curves are very "close," but the differential signatures are not. See Figure 2.6. The differential signatures for the

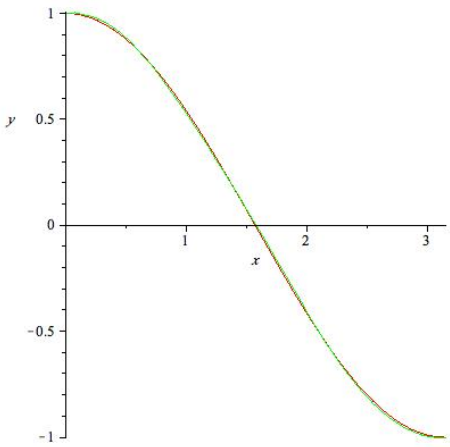

Figure 2.5: Graph of $\gamma = (t, \cos t)$ and its small perturbation given in (2.5)

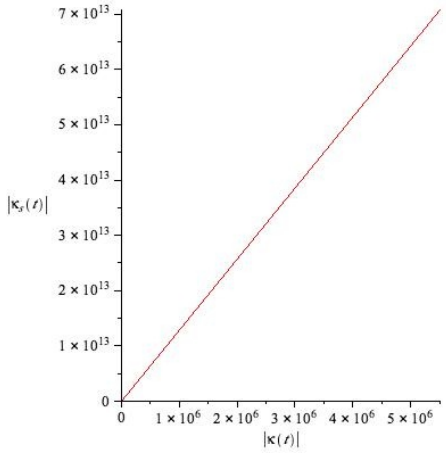

Figure 2.6: Euclidean differential signature for a small perturbation of $\gamma = (t, \cos t)$ computed using exact formula

cosine curve and a small perturbation of the cosine curve in Figures 2.2 and 2.6 are computed using explicit formulas. Because we use explicit formulas to compute the Euclidean differential signature for the perturbed curve, we capture high amplitude changes in curvature, and the range of κ and κ_s gets very large. If we discretize the curve, we get the Euclidean differential signature given in Figure 2.7. The range is much more reasonable because by sampling the curve, we miss some of the high frequency perturbation. The signature computed by sampling the perturbed curve still does not look like the differential signature for cosine.

We observe then that sensitivity to small perturbations make differential signatures impractical. In Chapter 3 we will consider integral signatures that are much less sensitive to small perturbations. We will begin by calculating integral invariants. We can use these integral invariants to define several global and local integral signatures. In Chapter 4, we will define a metric on the space of curves and their signatures to

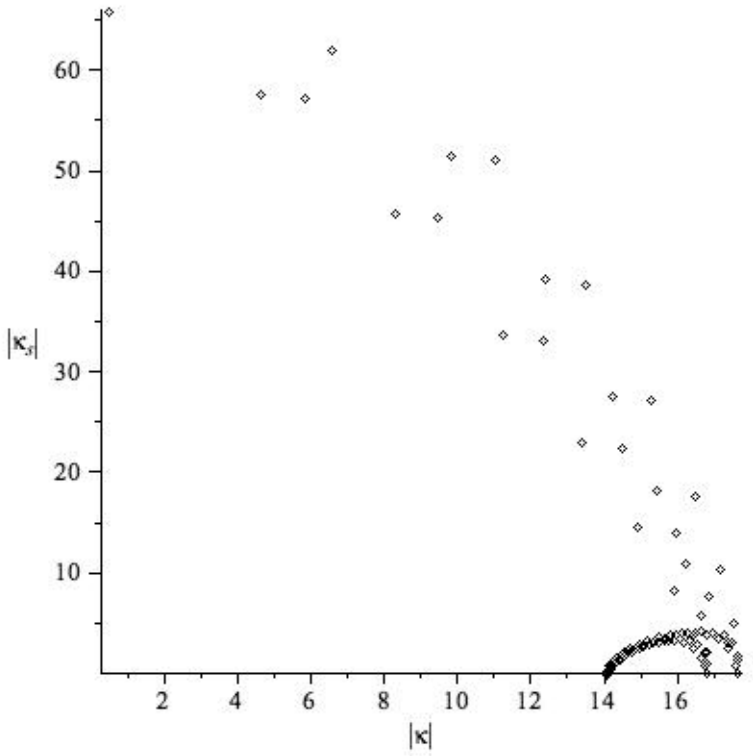

Figure 2.7: Euclidean differential signature for a small perturbation of $\gamma = (t, \cos t)$ computed by discrete approximation given in [14]

give a precise meaning to the word "close."

Chapter 3

Integral Signature

3.1 Integral Variables and Invariants

In this section we follow the presentation of [29] and [23] to define integral invariants for the action of the Euclidean and affine groups on curves in the plane. We will then use these to define Euclidean integral signatures for use in curve matching.

Let $(x(t), y(t))$ be a curve in $\mathbb{R}^2$, where $t \in [0, b]$ for some $b \neq 0 \in \mathbb{R}$. We will define integral variables in the following way:

$$\begin{aligned} x^{(ij)}(t) &= \int_0^t x^i(\tau) y^j(\tau) dx(\tau) \\ y^{(ij)}(t) &= \int_0^t x^i(\tau) y^j(\tau) dy(\tau). \end{aligned} \tag{3.1}$$

The order of the integral variables is $i + j$. To calculate integral invariants, we will only need integral variables up to second order.

Furthermore, we will only need to consider the following integral variables:

$$\begin{aligned} y^{(10)}(t) &= \int_0^t x(\tau)dy(\tau) \\ y^{(11)}(t) &= \int_0^t x(\tau)y(\tau)dy(\tau) \\ x^{(11)}(t) &= \int_0^t x(\tau)y(\tau)dx(\tau). \end{aligned} \tag{3.2}$$

The other second order integral variables can be written in terms of $x(t), y(t), y^{(10)}(t)$, $y^{(11)}(t)$, and $x^{(11)}(t)$ using integration by parts. For instance, we can rewrite $x^{(01)}(t)$ as follows.

$$\begin{aligned} x^{(01)}(t) &= \int_0^t y(\tau)dx(\tau) \\ &= x(t)y(t) - x(0)y(0) - \int_0^t x(\tau)dy(\tau) \\ &= x(t)y(t) - x(0)y(0) - y^{(10)}(t). \end{aligned} \tag{3.3}$$

For the curve $(x(t), y(t))$, the Euclidean transformations can be written in the following way.

$$\begin{aligned} \bar{x}(t) &= \cos(\phi)x(t) - \sin(\phi)y(t) + a \\ \bar{y}(t) &= \epsilon(\sin(\phi)x(t) + \cos(\phi)y(t) + b), \end{aligned} \tag{3.4}$$

where $\phi, a, b \in \mathbb{R}$ and $\epsilon = \pm 1$.

We prolong this action to the variables $y^{(10)}(t)$, $y^{(11)}(t)$, and $x^{(11)}(t)$. We show the

calculations for $\bar{y}^{(10)}(t)$. The other calculations are done in a similar manner.

$$\begin{aligned}
\bar{y}^{(10)}(t) &= \int_0^t \bar{x}(\tau) d\bar{y}(\tau) \\
&= \int_0^t (\cos(\phi)x(\tau) - \sin(\phi)y(\tau) + a) d(\sin(\phi)x(\tau) + \cos(\phi)y(\tau) + b) \\
&= \frac{\cos(\phi)\sin(\phi)}{2}[x^2(t) - x^2(0) - y^2(t) + y^2(0)] \\
&+ \cos^2(\phi)y^{(10)}(t) - \sin^2(\phi)x^{(01)}(t) \\
&= y^{(10)}(t) + \frac{\cos(\phi)\sin(\phi)}{2}[x^2(t) - x^2(0) - y^2(t) + y^2(0)] \\
&- \sin^2(\phi)[x(t)y(t) - x(0)y(0)]
\end{aligned}$$

We will introduce new variables:

$$\begin{aligned}
X(t) &= x(t) - x(0) \\
Y(t) &= y(t) - y(0).
\end{aligned} \tag{3.5}$$

Using these variables, we consider the 5-dimensional space with coordinates $(X(t), Y(t), Y^{(10)}(t), Y^{(11)}(t), X^{(11)}(t))$. By making the translation to the origin, we simplify the problem to finding integral invariants for the action:

$$\begin{aligned}
\bar{X}(t) &= \cos(\phi)X(t) - \sin(\phi)Y(t) \\
\bar{Y}(t) &= \sin(\phi)X(t) + \cos(\phi)Y(t) \\
\bar{Y}^{(10)}(t) &= Y^{(10)}(t) + \frac{1}{2}\cos\phi\sin\phi(X^2(t) - Y^2(t)) - \sin^2\phi X(t)Y(t) \\
\bar{Y}^{(11)}(t) &= \cos\phi Y^{(11)}(t) - \sin\phi X^{(11)}(t) + \frac{1}{3}\cos\phi\sin\phi[\sin\phi X^3(t) \\
&+ 3\cos\phi X^2(t)Y(t) - 3\sin\phi X(t)Y^2(t) - \cos\phi Y^3(t)] \\
\bar{X}^{(11)}(t) &= \cos\phi X^{(11)}(t) + \sin\phi Y^{(11)}(t) + \frac{1}{3}\cos\phi\sin\phi[\cos\phi X^3(t) \\
&- 3\sin\phi X^2(t)Y(t) - 3\cos\phi X(t)Y^2(t) + \sin\phi Y^3(t)].
\end{aligned} \tag{3.6}$$

In [23], Feng, Kogan, and Krim calculate the following integral invariants:

$$\begin{aligned}
R(t) &= \sqrt{X^2(t) + Y^2(t)} \\
I_1(t) &= Y^{(10)}(t) - \frac{1}{2}X(t)Y(t) \\
I_2(t) &= Y^{(11)}(t)X(t) - \frac{1}{2}Y^{(20)}(t)Y(t) - \frac{1}{6}X^2(t)Y^2(t)
\end{aligned} \tag{3.7}$$

The invariant I_2 can be rewritten as

$$X(t)Y^{(11)}(t) - \frac{1}{2}X^2(t)Y(t) + \frac{1}{2}Y(t)X^{(11)}(t) - \frac{1}{6}X^2(t)Y^2(t),$$

using integration by parts. Distance R is invariant under the Euclidean action, while I_1 and I_2 are invariants under the special affine action. The invariant I_1 has a straightforward geometric interpretation, shown in Figure 3.1 [23].

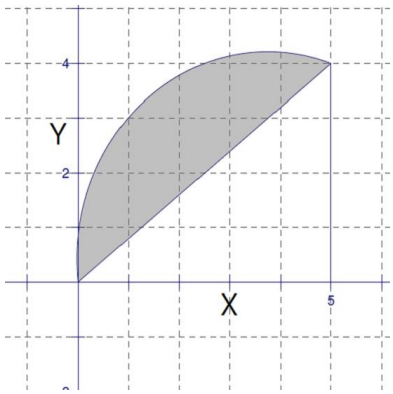

Figure 3.1: Geometric interpretation of I_1

For a curve $(X(t), Y(t))$, shifted to the origin, $\frac{1}{2}X(t)Y(t)$ is the area of the right triangle with hypotenuse from $(0, 0)$ to the point $(X(t), Y(t))$ for some $t \in \mathbb{R}$. The term $Y^{(10)}(t)$ refers to the area under the curve from 0 to a real number t. Then $I_1(t)$ corresponds to the area of the shaded region in Figure 3.1 at each point $(X(t), Y(t))$.

The invariant I_2 has a somewhat more involved geometric interpretation. See [23] for details.

3.2 Discrete Approximation of Invariants

We will apply integral invariants to discrete images and thus will need discrete approximations of the invariants. We use the trapezoid rule for a discrete approximation of I_1. The formula for this approximation is

$$I_1(n) = \sum_{j=1}^{n} \frac{Y_j + Y_{j-1}}{2}(X_j - X_{j-1}) - \frac{X(n)Y(n)}{2}. \tag{3.8}$$

We prove that the approximation of I_1 is invariant under the special affine group,

and therefore under its subgroup, the special Euclidean group.

Theorem 3.2.1. *The approximation of I_1 is invariant under the action of the special affine group, $SA(2)$.*

Proof. Invariance under translation is achieved by shifting the initial point of the curve to the origin. It is then sufficient to prove that equation (3.8) is invariant with respect to the action of $SL(2)$.

Consider the case where $n = 2$. Then the formula for $I_1(2)$ is

$$I_1(2) = \frac{1}{2}[(X_1 - X_0)(Y_1 + Y_0) + (X_2 - X_1)(Y_2 + Y_1) - X_2Y_2].$$

Expanding this out gives us

$$\frac{1}{2}(X_1Y_1 + X_1Y_0 - X_0Y_1 - X_0Y_0 + X_2Y_2 + X_2Y_1 - X_1Y_2 - X_1Y_1 - X_2Y_2).$$

Canceling terms and using the fact that (X_0, Y_0) is equal to the origin, we end up with $\frac{1}{2}(X_1Y_0 - X_0Y_1 + X_2Y_1 - X_1Y_2)$. Notice that $X_1Y_0 - X_0Y_1 = 0$, and the last two terms correspond to

$$-\frac{1}{2}\begin{vmatrix} X_1 & X_2 \\ Y_1 & Y_2 \end{vmatrix}.$$

This term is invariant under $SL(2)$ because determinants are invariant under this action.

Similarly, for a general value of n,

$$I_1(n) = -\frac{1}{2}\sum_{j=1}^{n}\begin{vmatrix} X_{j-1} & X_j \\ Y_{j-1} & Y_j \end{vmatrix}.$$

Therefore, the approximation of I_1 is invariant under $SL(2)$. □

Up to sign, the approximation of $I_1(n)$ is the sum of the areas of the triangles shown in Figure 3.2. The area of a triangle is invariant under the action of $SL(2)$.

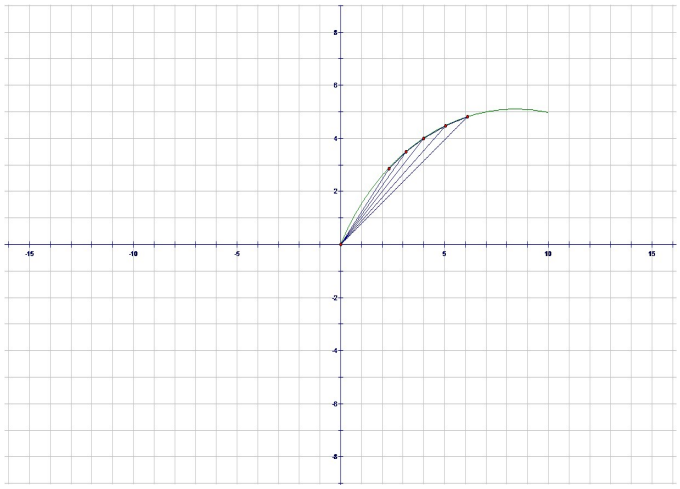

Figure 3.2: Approximation of invariant I_1

This is not the case for the discrete approximation of I_2, which is given by

$$\begin{aligned} I_2(n) &= -X^2(n)Y^2(n) + \frac{3}{2}X(n)\sum_{j=1}^{n}\left(\frac{Y_j + Y_{j-1}}{2}\right)^2 (X_j - X_{j-1}) \\ &+ \frac{3}{2}Y(n)\sum_{j=1}^{n}\left(\frac{X_j + X_{j-1}}{2}\right)^2 (Y_j - Y_{j-1}). \end{aligned}$$

Consider the cosine curve on $[0, \pi]$ and a rotation of cosine by $\frac{\pi}{4}$. We will use 10 partitions to approximate I_2. In Table 3.1 We give $I_2(n)$ with $N = 10$ partitions of the interval $[0, \pi]$.

Table 3.1: $I_2(n)$ for $\gamma = (t, \cos t)$ and a rotation with $N = 10$ partitions of $t \in [0, \pi]$

	Cosine Curve	Rotation of Cosine
$I_2(1)$	0	0
$I_2(2)$	-0.0001	-0.0008
$I_2(3)$	-0.0007	-0.0018
$I_2(4)$	0.0011	0.0016
$I_2(5)$	0.0119	0.0164
$I_2(6)$	0.0385	0.0491
$I_2(7)$	0.0835	0.1022
$I_2(8)$	0.1413	0.1697
$I_2(9)$	0.1932	0.2327
$I_2(10)$	0.2079	0.2588

Now suppose we use 100 partitions. We will compare 10 of the values for $I_2(n)$.

Table 3.2: $I_2(n)$ for $\gamma = (t, \cos t)$ and a rotation with $N = 100$ Partitions of $t \in [0, \pi]$

	Cosine Curve	Rotation of Cosine
$I_2(10)$	1.5357e-05	7.4927e-06
$I_2(20)$	0.001	0.000992
$I_2(30)$	0.0081	0.0081
$I_2(40)$	0.0303	0.0304
$I_2(50)$	0.0751	0.0753
$I_2(60)$	0.1429	0.1432
$I_2(70)$	0.2201	0.2205
$I_2(80)$	0.2735	0.2740
$I_2(90)$	0.2661	0.2668
$I_2(100)$	0.2896	0.2903

As the total number, N, of partitions tends to ∞, the approximation of I_2 becomes invariant.

3.3 Global Integral Signatures

Definition 3.3.1. *The* **signature** *of a curve is a plane curve parametrized by two invariants.*

For a curve $\gamma(t)$, we can define signatures based on invariants $R(t), I_1(t)$, and $I_2(t)$. Namely, we define the signatures:

- $(R(t), I_1(t))$,
- $(R(t), I_2(t))$,
- $(I_1(t), I_2(t))$.

These signatures are called global because their computations involve integration along the entire curve. In [1], we showed that $(R(t), I_1(t))$ classifies curves up to $SE(2)$ and that $(R(t), I_2(t))$ classifies curves up to $A(2)$. In [23], $(I_1(t), I_2(t))$ was used to classify curves up to affine transformations. We will reproduce the proofs from [1].

Theorem 3.3.2. *Let γ and $\bar{\gamma}$ be two continuously differentiable curves such that for each $r > 0$, γ and $\bar{\gamma}$ intersect a circle of radius r at most once. Then γ and $\bar{\gamma}$ are equivalent with respect to $SE(2)$ if their $(R(t), I_1(t))$ signatures coincide.*

Proof. In order to prove this statement, it is more convenient to use polar coordinates. Let γ be given by $\theta = \phi(R)$ and $\bar{\gamma}$ given by $\theta = \bar{\phi}(R)$. Using translation, we can assume that the initial point is zero, and so it is sufficient to prove the theorem for rotations. In polar coordinates $I_1^{\gamma}(R)$ is given by:

$$I_1^{\gamma}(R) = \frac{1}{2}\int_{R_0}^{R} R^2 \frac{d\phi}{dR} dR. \tag{3.9}$$

Suppose that γ and $\bar{\gamma}$ are related by a rotation. Then $\bar{\phi} = \phi + \theta_0$ for $\theta_0 \in \mathbb{R}$. We will show that $I_1^{\gamma}(R) = I_1^{\bar{\gamma}}(R)$. Indeed, using equation (3.9), we obtain:

$$\begin{aligned} I_1^{\bar{\gamma}}(R) &= \frac{1}{2}\int_{R_0}^{R} R^2 \frac{d\bar{\phi}}{dR} dR \\ &= \frac{1}{2}\int_{R_0}^{R} R^2 \frac{d(\phi + \theta_0)}{dR} dR \\ &= \frac{1}{2}\int_{R_0}^{R} R^2 \frac{d\phi}{dR} dR \end{aligned}$$

Thus the $(R, I_1(R))$ signatures coincide.

Now assume that $I_1^{\gamma}(R) = I_1^{\bar{\gamma}}(R)$ for the curves γ and $\bar{\gamma}$. We must show that $\bar{\phi} = \phi + \theta_0$ for $\theta_0 \in \mathbb{R}$.

$$I_1^{\gamma}(R) = I_1^{\bar{\gamma}}(R) \quad \Longrightarrow \quad \frac{1}{2}\int_{R_0}^{R} R^2 \left(\frac{d\bar{\phi}}{dR} - \frac{d\phi}{dR}\right) dR = 0. \tag{3.10}$$

Differentiating 3.10 with respect to R gives us $R^2 \frac{d(\bar{\phi}-\phi)}{dR} = 0$. Then $\frac{d(\bar{\phi}-\phi)}{dR} = 0$, which implies that $\bar{\phi} = \phi + \theta_0$ for $\theta_0 \in \mathbb{R}$. Therefore γ and $\bar{\gamma}$ are related by a rotation. □

Theorem 3.3.3. *Suppose γ and $\bar{\gamma}$ are continuously differentiable curves such that for each $r > 0$, γ and $\bar{\gamma}$ intersect a circle of radius r at most once. Then γ and $\bar{\gamma}$ are equivalent with respect to $A(2)$ if their (R, I_2) signatures coincide.*

Proof. Again, we will use polar coordinates to prove this theorem. As in the proof of

Theorem 3.3.2, let us assume that γ is given by $\theta = \phi(R)$ and $\bar{\gamma}$ is given by $\theta = \bar{\phi}(R)$.

In polar coordinates, $I_2^{\gamma}(R)$ is given by:

$$I_2^{\gamma}(R) = R\sin\theta \int_{R_0}^{R} R^3 \cos\theta \frac{d\theta}{dR} dR - R\cos\theta \int_{R_0}^{R} R^3 \sin\theta \frac{d\theta}{dR} dR. \tag{3.11}$$

As seen in the proof of Theorem 3.3.2, it is a fairly straightforward exercise to show that if γ and $\bar{\gamma}$ are related by a rotation or reflection, then their $(R, I_2(R))$ signatures coincide.

We want to show that if $I_2^{\gamma}(R) = I_2^{\bar{\gamma}}(R)$, then γ and $\bar{\gamma}$ are related by a rotation or reflection. We will begin by dividing $I_2(R)$ by R and then differentiating with respect to R. This gives us the equation:

$$\frac{d}{dR}\frac{I_2^{\gamma}(R)}{R} = \cos\phi \frac{d\phi}{dR} \int_{R_0}^{R} R^3 \cos\phi \frac{d\phi}{dR} dR + \sin\phi \frac{d\phi}{dR} \int_{R_0}^{R} R^3 \sin\phi \frac{d\phi}{dR} dR. \tag{3.12}$$

We will simplify the proof by introducing the following notation.

$$\begin{aligned} V_1 &= \int_{R_0}^{R} R^3 \cos\phi \frac{d\phi}{dR} dR \\ V_2 &= \int_{R_0}^{R} R^3 \sin\phi \frac{d\phi}{dR} dR \\ \overline{V_1} &= \int_{R_0}^{R} R^3 \cos\bar{\phi} \frac{d\bar{\phi}}{dR} dR \\ \overline{V_2} &= \int_{R_0}^{R} R^3 \sin\bar{\phi} \frac{d\bar{\phi}}{dR} dR \end{aligned}$$

Since $\frac{I_2^{\gamma}(R)}{R} = \frac{I_2^{\bar{\gamma}}(R)}{R}$, we have the equality:

$$\sin\phi V_1 - \cos\phi V_2 = \sin\overline{\phi V_1} - \cos\overline{\phi V_2}. \tag{3.13}$$

From 3.12, we obtain

$$\frac{d\phi}{dR}(\cos\phi V_1 + \sin\phi V_2) = \frac{d\bar{\phi}}{dR}(\cos\overline{\phi V_1} + \sin\overline{\phi V_2}). \tag{3.14}$$

To show that γ and $\bar{\gamma}$ are related by a rotation or reflection, we must show that $\frac{d\bar{\phi}}{d\phi} = \pm 1$. We will calculate $\frac{d\bar{\phi}}{d\phi}$ and its square. Using the chain rule and equation (3.14), we get:

$$\frac{d\bar{\phi}}{d\phi} = \frac{\frac{d\bar{\phi}}{dR}}{\frac{d\phi}{dR}} = \frac{\cos\phi V_1 + \sin\phi V_2}{\cos\overline{\phi V_1} + \sin\overline{\phi V_2}} \tag{3.15}$$

$$\left(\frac{d\bar{\phi}}{d\phi}\right)^2 = \frac{V_1^2 + V_2^2 - (\sin\phi V_1 - \cos\phi V_2)^2}{\overline{V_1}^2 + \overline{V_2}^2 - (\sin\overline{\phi V_1} - \cos\overline{\phi V_2})^2} \tag{3.16}$$

From 3.13 and 3.16, it follows that $\left(\frac{d\bar{\phi}}{d\phi}\right)^2 = 1$ if $\overline{V_1}^2 + \overline{V_2}^2 - (V_1^2 + V_2^2) = 0$. At R_0, we have $V_1, V_2, \overline{V_1}$, and $\overline{V_2}$ equal to zero. Then $\frac{d\bar{\phi}}{d\phi} = \pm 1$, and we conclude that γ and $\bar{\gamma}$ are related by a rotation or reflection. □

3.3.1 Some Properties of the Global (R, I_1) Signature

Robustness to Small Perturbations We make several observations about the (R, I_1) signature. The first observation is that the (R, I_1) signature is much less sen-

sitive to the effects of a small perturbation. Recall in Chapter 2, Example 2.2.3, the curves γ and $\tilde{\gamma}$ are given by Equations (2.4) and (2.5). This example illustrated that the differential signatures for γ and $\tilde{\gamma}$ are very sensitive to small perturbations. Figure 3.3 shows the (R, I_1) integral signature for the same curves. We note that the integral signature of $\tilde{\gamma}$ is not very different from the integral signature of γ.

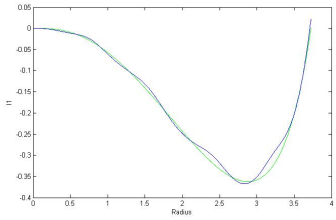

Figure 3.3: (R, I1) Signature for $\gamma = (t, \cos t)$ and its perturbation $\tilde{\gamma}$ given by equation (2.5)

The signature curves are "close." In order to define what is meant by "close," we will need to put a metric on the space of curves and their signature curves. We will define and study a metric on the space of signature curves in Chapter 4. The distance between signature curves may also be referred to as the distance between congruence classes.

Dependence on Initial Points The (R, I_1) signature is defined for the entire curve and is dependent on the initial point. This may be problematic in the case where there is not a clearly defined initial point, as in the following example.

Example 3.3.4. *Consider the three leaf rose, given in polar coordinates by* $(\theta = t, r = \cos(3t))$.

The choice of initial point for this curve is arbitrary and will affect the signature

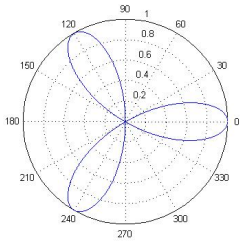

Figure 3.4: Three leaf rose

curve. Suppose we choose an initial point of $(0, 1)$ *and an initial point of* $(0, 0)$*. We get the signature curves shown in Figures 3.5 and 3.6.*

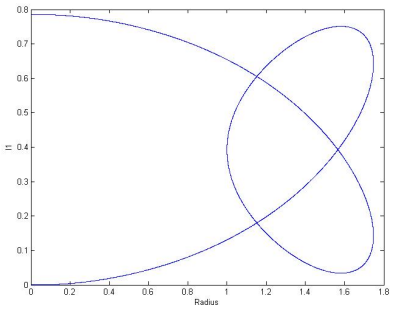

Figure 3.5: (R, I_1) for three leaf rose starting at $(0, 1)$

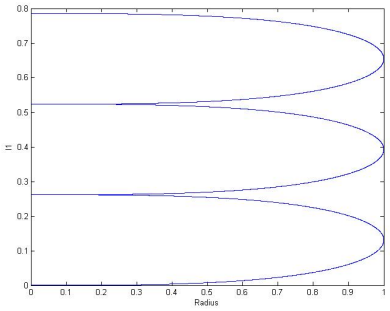

Figure 3.6: (R, I_1) for three leaf rose starting at $(0, 0)$

Later in this chapter we will look at a local signature that is independent of the choice of initial point.

Effects of Reflectional Symmetry of the Original Curve on its Signature Recall that the (R, I_1) signature classifies curves up to rotations and translations. We note however that if a curve is reflected, its (R, I_1) signature is also reflected.

Example 3.3.5. *Let $\gamma = (t, e^t)$ on $[0, 1]$, and let $\bar{\gamma} = (-t, e^t)$ on $[0, 1]$. The signature curves for γ and $\tilde{\gamma}$ are shown in Figures 3.7 and 3.8.*

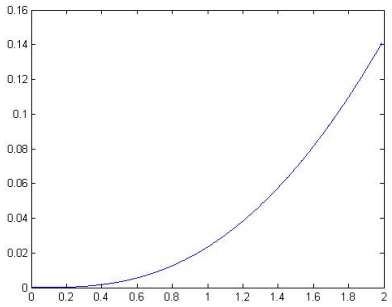

Figure 3.7: (R, I_1) for $\gamma = (t, e^t)$

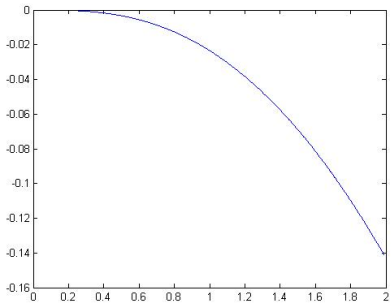

Figure 3.8: (R, I_1) for $\bar{\gamma} = (-t, e^t)$

As a result of this property, if an image has reflectional symmetry, then its signature curve will also have reflectional symmetry. For example, the signature curve in Figure 3.5 is symmetric.

Effects of Multiple Tracings of the Original Curve on its Signature When a curve is traced multiple times, the (R, I_1) signature is periodic. Consider the three leaf rose on $[0, \pi]$ traced twice. We get the (R, I_1) signature shown in Figure 3.9.

This will occur regardless of the choice of initial point.

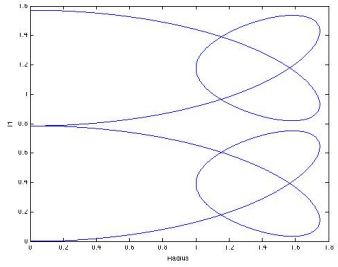

Figure 3.9: (R, I_1) for three leaf rose traced twice

3.3.2 Some Properties of the Global (R, I_2) Signature

Robustness to Small Perturbations As with the (R, I_1) signature, we see that the (R, I_2) signature for a curve is less affected by a small perturbation than the differential signature.

Example 3.3.6. *Consider* $\gamma = (t, \cos t)$ *for* $t \in [0, \pi]$ *and a small perturbation of* γ. *We get the following signature curves.*

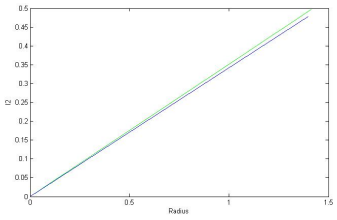

Figure 3.10: (R, I_2) for $\gamma = (t, \cos t)$ and a small perturbation

Dependence on Initial Point The (R, I_2) signature for a curve depends on the chosen initial point, as is the case for the (R, I_1) signature. Consider the following example.

Example 3.3.7. *Let $\gamma = (\theta, \cos(3\theta))$ for $\theta \in [0, \pi]$, with initial point $(0, 1)$. Then the (R, I_2) signature is given by Figure 3.11.*

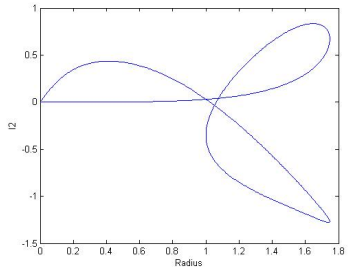

Figure 3.11: (R, I_2) for three leaf rose with initial point $(0, 1)$

Now use the same γ but with $\theta \in [\frac{\pi}{2}, \frac{3\pi}{2}]$ and initial point $(0, 0)$, whose signature is given in Figure 3.12.

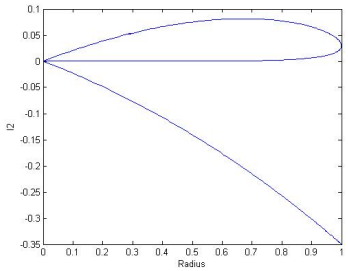

Figure 3.12: (R, I_2) for three leaf rose with initial point $(0, 0)$

Effects of Multiple Tracings of the Original Curve on its Signature

Example 3.3.8. *Let γ be the three leaf rose with (R, I_2) signature given in Figure 3.11. If we trace the three leaf rose three times, it begins to "fill in" as seen in Figure 3.13.*

One would expect the (R, I_2) signature to show periodicity when the original cure is traced multiple times, and in fact it does, by "filling in." The "filling in" occurs when

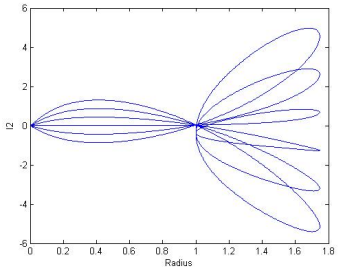

Figure 3.13: (R, I_2) for three leaf rose traced three times

the rose is traced multiple times because the first tracing of the signature curve does not end exactly at $I_2 = 0$.

3.4 Local Integral Invariants and Signatures

The invariants I_1 and I_2 require integration along the entire curve. Signatures based on these invariants then are global, thus cannot be used for local comparisons. For instance, global invariants cannot be used to detect occlusions. In [23], the authors use local signatures for classifying curves up to $A(2)$. We will consider the local (I_1^{loc}, I_2^{loc}) signature for the action of the Euclidean group. We obtain local invariants by restricting I_1 and I_2 to subintervals.

In order to compute the local (I_1^{loc}, I_2^{loc}) signature for a curve, we take the following steps.

- Divide the curve into m equal intervals, Δ_l for $l = 1, \ldots, m$ of equal length.
- Approximate $I_1^{loc}(l)$ and $I_2^{loc}(l)$ on each interval, using formulas 3.17 and 3.18.
- Then the signature (I_1^{loc}, I_2^{loc}) is defined as $\{(I_1^{loc}(l), I_2^{loc}(l)) | l = 1, \ldots, m\}$

$$
\begin{aligned}
I_1^{loc}(l) &= \frac{\left(X(l+1)-X(l)\right)\left(Y(l+1)-Y(l)\right)}{2} \qquad (3.17)\\
&- \sum_{j=1}^{N}\left(\frac{Y_{j,(l+1)}+Y_{j,l}}{2}-Y_l\right)\left(X_{j,(l+1)}-X_{j,l}\right)\\
I_2^{loc}(l) &= -\left(X_{(l+1)}-X_l\right)^2\left(Y_{(l+1)}-Y_l\right)^2 \qquad (3.18)\\
&+ \frac{3}{2}\left(X_{(l+1)}-X_l\right)\sum_{j=1}^{N}\frac{\left(Y_{j-1,l}-Y_l\right)^2+\left(Y_{j,l}-Y_l\right)^2}{2}\left(X_{j,l}-X_{(j-1),l}\right)\\
&+ \frac{3}{2}\left(Y_{(l+1)}-Y_l\right)\sum_{j=1}^{N}\frac{\left(X_{j-1,l}-X_l\right)^2+\left(X_{j,l}-X_l\right)^2}{2}\left(Y_{j,l}-Y_{(j-1),l}\right),
\end{aligned}
$$

where N is the number of partitions of intervals, Δ_l, used to approximate the integrals.

We can define two other Euclidean signatures based on local integral invariants, namely:

- $(l, I_1^{loc}(l))$ for $l = 1, \ldots, m$.
- $(l, I_2^{loc}(l))$ for $l = 1, \ldots, m$.

Observe that the signatures $(l, I_1^{loc}(l)), (l, I_2^{loc}(l)),(I_1^{loc}, I_2^{loc})$ classify curves up to the Euclidean group even though I_1, I_2 are affine integral invariants. This is because we use the Euclidean invariant R to partition the curve into equal length intervals. In addition to dividing the curve into intervals, we shift the initial point of each interval to the origin. The advantage to using local integral signatures is that they can detect occlusions. The local signatures depend on choice of m and N.

3.4.1 Properties of $(l, I_1^{loc}(l))$ and $(l, I_2^{loc}(l))$ Signatures

These are local signatures and allow comparison of images with occlusions. These signatures depend on selection of initial point in a predictable way. For different initial points, the signatures will be the same up to translation. The advantage of $(l, I_1^{loc}(l))$ is that the approximation of $I_1^{loc}(l)$ is invariant under $SE(2)$. The $(l, I_1^{loc}(l))$ signature may be particularly useful when there is a clearly identified initial point.

Dependence on Initial Points We will consider the $(l, I_1^{loc}(l))$ and $(l, I_2^{loc}(l))$ signature curves for a three leaf rose with different initial points. See Figures 3.14 through 3.17

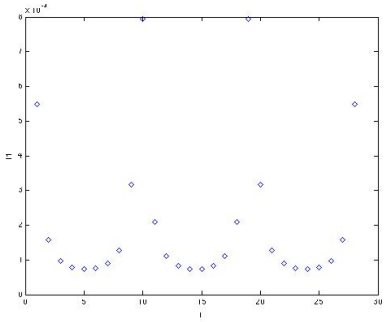

Figure 3.14: $(l, I_1^{loc}(l))$ for three leaf rose with initial point $(0, 1)$

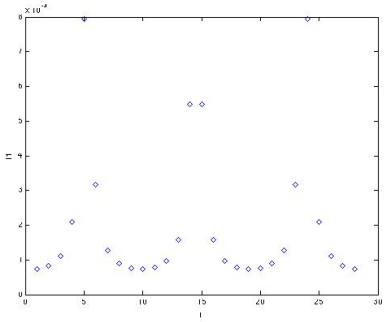

Figure 3.15: $(l, I_1^{loc}(l))$ for three leaf rose with initial point $(0, 0)$

Effects of Reflectional Symmetry of the Original Curve on its Signature The $(l, I_1^{loc}(l))$ and $(l, I_2^{loc}(l))$ signatures have the same properties with the exception of the effect of reflection of the initial curve. Recall that I_1 changes sign when the curve is reflected, and I_2 remains invariant with respect to reflection. If the original curve

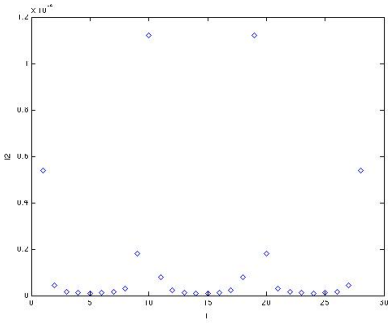

Figure 3.16: $(l, I_2^{loc}(l))$ for three leaf rose with initial point $(0, 1)$

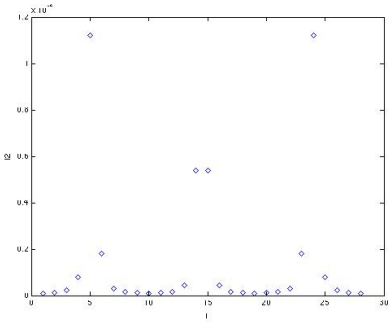

Figure 3.17: $(l, I_2^{loc}(l))$ for three leaf rose with initial point $(0, 0)$

is reflected about a line, then the $(l, I_1^{loc}(l))$ signature is reflected, and the $(l, I_2^{loc}(l))$ signature remains the same.

Let γ be the reflection of the three leaf rose about the y-axis. Observe the signature curves for γ and its reflection, given in Figures 3.18 and 3.19.

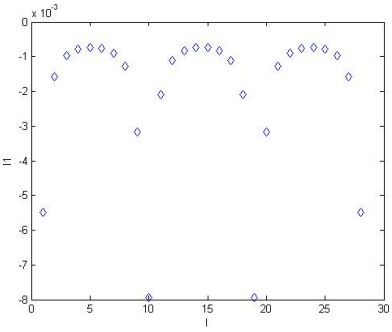

Figure 3.18: $(l, I_1^{loc}(l))$ for three leaf rose reflected about the y-axis

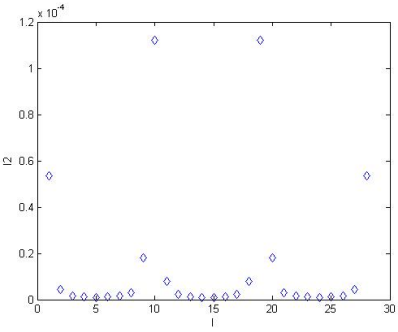

Figure 3.19: $(l, I_2^{loc}(l))$ for three leaf rose reflected about the y-axis

Rotational Symmetry of Original Curve Consider the $(l, I_1^{loc}(l))$ signature for one leaf of the three leaf rose. If we trace the entire three leaf rose using the same choice of initial point, the signature will become periodic. See Figures 3.20 and 3.21.

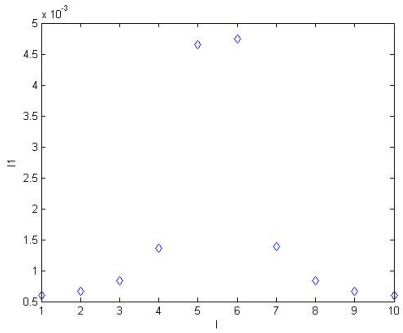

Figure 3.20: $(l, I_1^{loc}(l))$ for one leaf of the three leaf rose

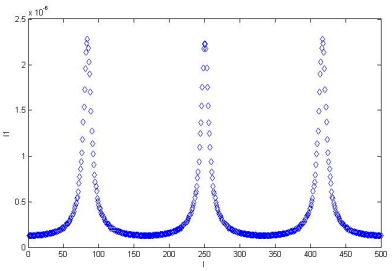

Figure 3.21: $(l, I_1^{loc}(l))$ for three leaf rose

3.4.2 Properties of (I_1^{loc}, I_2^{loc}) Signature

The dependence of $(l, I_1^{loc}(l))$ and $(l, I_2^{loc}(l))$ on initial point is problematic because some curves do not have an obvious initial point. We wish to eliminate the dependence on initial point and do so by considering the local (I_1^{loc}, I_2^{loc}) signature. This local signature does not depend on the choice of initial point.

We demonstrate the independence of choice of initial point using the three leaf rose.

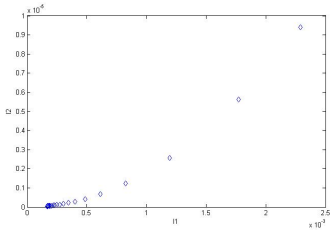

Figure 3.22: (I_1^{loc}, I_2^{loc}) for three leaf rose with initial points $(0, 1)$ and $(0, 0)$

Notice that the three leaf rose has rotational symmetry. The (I_1^{loc}, I_2^{loc}) signatures for a single leaf and for the entire three leaf rose are the same.

In the next chapter, we will discuss how to define the distance between congruence

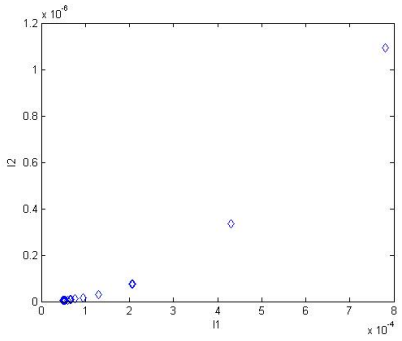

Figure 3.23: (I_1^{loc}, I_2^{loc}) for three leaf rose

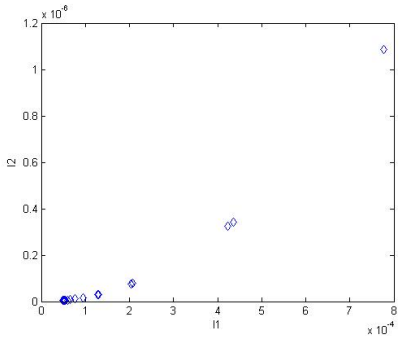

Figure 3.24: (I_1^{loc}, I_2^{loc}) for one leaf of the three leaf rose

classes. We will restrict our focus to the (I_1^{loc}, I_2^{loc}) signature. We can make this signature invariant with respect to the similarity group by considering how the scaling:

$$x \mapsto \lambda x$$

$$y \mapsto \lambda y,$$

where $\lambda \in \mathbb{R}$, $\lambda \neq 0$, affects I_1 and I_2. It is shown in [23] that

$$\overline{I_1^{loc}} = \frac{I_1^{loc}}{max|I_1^{loc}|} \tag{3.19}$$

$$\overline{I_2^{loc}} = \frac{I_2^{loc}}{max[(I_1^{loc})^2]} \tag{3.20}$$

are invariant with respect to the similarity group.

We will now examine the use of distance in curve matching and define what is meant by "close."

Chapter 4

Distance Between Congruence Classes of Curves

4.1 A Metric on the Space of Curves and Their Congruence Classes

We noted in Chapter 3 that the integral signatures of a curve and its perturbations are "close." Now we must define a distance between the original curves. Let $\mathcal{C}$ be the space of continuous curves in $\mathbb{R}^2$.

Definition 4.1.1. *A function $d : \mathcal{C} \times \mathcal{C} \to \mathbb{R}$ is a distance function if for all $\gamma_1, \gamma_2, \gamma_3 \in \mathcal{C}$ the following conditions are satisfied:*

1. $d(\gamma_1, \gamma_2) \geq 0$,
2. $d(\gamma_1, \gamma_2) = d(\gamma_2, \gamma_1)$,

3. $\gamma_1 = \gamma_2 \iff d(\gamma_1, \gamma_2) = 0$, *and*

4. $d(\gamma_1, \gamma_3) \leq d(\gamma_1, \gamma_2) + d(\gamma_2, \gamma_3)$.

Given two parametric curves, $\gamma_1(t) = (x(t), y(t))$ for $t \in I_{\gamma_1}$ and $\gamma_2 = (x(\tau), y(\tau))$ for $\tau \in I_{\gamma_2}$, one could use a variation of the L^p norm to define a distance between these curves. Using the L^p norm to define distance would require a synchronization of their parametrizations, $t = h(\tau)$, and the distance will depend on the choice of h. One can use the arc length parameter to match parametrizations, but in practice, parametrizing a curve by arc length may be very difficult. Another issue with using the above distance is that the two curves may not have the same arc length. Lastly, parametrization with respect to arc length depends on the choice of initial point, which may not be clearly defined for closed curves.

If we instead use Hausdorff distance, we do not need to define the correspondence between parametrizations. Also, the Hausdorff distance does not depend on the initial point of the curve. For examples of applications of Hausdorff distance in computer vision, see [33] and [66]. Hausdorff distance is defined as follows.

Definition 4.1.2. *For curves* $\gamma_1(t), \gamma_2(t) \in \mathbb{R}^2$ *and points* $p_1 \in \gamma_1(t), p_2 \in \gamma_2(t)$, *the Hausdorff distance* $d_H(\gamma_1(t), \gamma_2(t))$ *is equal to* $\max(d_{H_1}, d_{H_2})$, *where*

$$d_{H_1} = \sup_{p_2 \in \gamma_2} \inf_{p_1 \in \gamma_1} ||p_1 - p_2|| \tag{4.1}$$

$$d_{H_2} = \sup_{p_1 \in \gamma_1} \inf_{p_2 \in \gamma_2} ||p_1 - p_2||, \tag{4.2}$$

where $||p_1 - p_2||$ is the usual Euclidean distance between two points in $\mathbb{R}^2$.

In Figure 4.1, d_{H_1} is the infimum of the δ's as the point p_1 moves along γ_1.

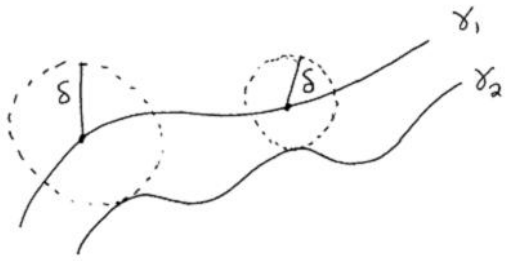

Figure 4.1: Illustration of δ_{H_1}

If one curve is related to another by a Euclidean transformation, the Hausdorff distance between the two curves may be very large. Our next step is to define a distance between congruence classes of curves.

Definition 4.1.3. *Let γ_1 and γ_2 be two continuous curves with integral signatures $\mathcal{S}_{\gamma_1}$ and $\mathcal{S}_{\gamma_2}$, respectively. Then the distance between equivalence classes $[\gamma_1]$ and $[\gamma_2]$ is defined as the Hausdorff distance between their signatures.*

$$\mathcal{D}([\gamma_1],[\gamma_2]) = d_H(\mathcal{S}_{\gamma_1},\mathcal{S}_{\gamma_2}). \tag{4.3}$$

If $\gamma_1 \cong \gamma_2$, then $\mathcal{S}_{\gamma_1} = \mathcal{S}_{\gamma_2}$. Hence $\mathcal{D}([\gamma_1],[\gamma_2]) = 0$, and $\mathcal{D}$ is indeed a distance between equivalence classes of curves. We conclude then that the distance between signature curves will give us the distance between congruence classes of curves.

Various signatures can be used to define the distance between congruence classes. We will restrict ourselves to examining the distance based on the $(\overline{I_1^{loc}}, \overline{I_2^{loc}})$ signature,

where $\overline{I_1^{loc}}$ and $\overline{I_2^{loc}}$ are local integral invariants for the similarity group as defined by Equations (3.19) and (3.20) in Chapter 3.

4.2 Experiments, Conclusions, and Future Work

Following the work in [39], we will look at images from the Kimia silhouette database [54] and compare shape images to small perturbations of those images. The Hausdorff distance between the original image and a small perturbation is 0.01. We now compare images and calculate the distance between congruence classes. Table 4.1 provides a small example. We look at images of an arctic hare, F-15, hand, and bonefish.

Table 4.1: Hausdorff distance between signatures for images

				
	**0.0339**	0.3893	0.2926	0.3385
	0.3944	**0.0374**	0.3156	0.3422
	0.2974	0.3011	**0.0189**	0.3278
	0.3472	0.3498	0.3477	**0.0382**

Notice that the smallest distances in Table 4.1, given in bold, are along the diagonal. This reflects the fact that the signature for the arctic hare is closest to the signature for a small perturbation of the arctic hare.

Table 4.2: Distance between congruence classes of images

	Arctic Hare	Blacktail	Desert Cotton	Eastern Cotton	European Hare	F-15	F-16	Harrier	Mig	Phantom
Arctic Hare	**0.0339**	0.3915	0.4829	0.5430	0.3213	0.3893	0.4026	0.3575	0.4119	0.3912
Blacktail	0.3777	**0.0280**	0.3273	0.5996	0.3665	0.3253	0.3580	0.3356	0.4940	0.4636
Desert Cottontail	0.4633	0.3066	**0.0749**	0.4865	0.3963	0.3872	0.2820	*0.2684*	0.5207	0.3863
Eastern Cottontail	0.5236	0.5801	0.5397	**0.0225**	0.3318	0.4223	0.4492	*0.2897*	0.4595	0.5618
European Hare	0.3373	0.3689	0.4068	0.3778	**0.0363**	*0.1986*	0.3058	0.3078	0.4338	0.4097
F-15	0.3944	0.3156	0.3814	0.4431	*0.2234*	**0.0374**	0.2948	0.2821	0.4125	0.3716
F-16	0.4136	0.3440	0.2782	0.4558	0.2713	0.2904	**0.0541**	0.2994	0.3924	*0.2479*
Harrier	0.4053	0.3257	0.2823	0.2999	*0.2614*	0.2821	0.3298	**0.0374**	0.4498	0.4343
Mig	0.4191	0.4999	0.5160	0.4664	0.4505	0.4459	0.4036	0.4485	**0.0197**	0.5183
Phantom	0.3473	0.4921	0.4105	0.5746	0.4172	0.3758	*0.2485*	0.4463	0.4741	**0.0619**
Hand	0.2974	0.3407	0.4240	0.4192	0.2534	0.3011	0.3426	0.3120	0.5194	0.3400
Hand10	0.5549	0.6107	0.5689	0.3829	0.3648	0.4552	0.4490	0.2752	0.4917	0.5926
Hand90	0.6246	0.6817	0.6426	0.3658	0.4312	0.5214	0.5225	0.3517	0.3558	0.6632
Handbent1	0.3045	0.5163	0.4345	0.5986	0.4417	0.4001	0.3570	0.4707	0.5271	0.2988
Handbent2	0.3962	0.4049	0.4865	0.3883	0.2444	0.4081	0.3524	0.4288	0.2944	0.4574
Bonefish	0.3472	0.3169	0.4130	0.5021	0.3500	0.3498	0.3194	0.3459	0.5187	*0.2845*
Cardinal Fish	0.4381	0.4312	0.4333	0.3273	0.2603	0.2743	0.4214	0.3029	0.3469	0.5273
Dogfish Shark	1.0179	1.4042	1.3223	1.4865	1.3280	1.2879	1.0331	1.3577	1.3516	0.9274
Goat Fish	0.4224	0.3535	0.3888	0.5392	0.3264	0.3476	0.3700	0.3593	0.3002	0.2906
Herrings	0.4102	0.7837	0.7031	0.8667	0.7056	0.6669	0.4146	0.7357	0.7295	0.3087

Table 4.3: Distance for congruence classes of images continued

	Hand	Hand10	Hand90	Handbent1	Handbent2	Bone Fish	Cardinal Fish	Dogfish Shark	Goat Fish	Herrings
Arctic Hare	*0.2926*	0.5388	0.6453	0.3021	0.3810	0.3385	0.4233	1.0486	0.4145	0.4385
Blacktail	0.3512	0.5949	0.7027	0.5205	0.4054	*0.3171*	0.4276	1.3879	0.3307	0.7782
Dessert Cottontail	0.4277	0.4862	0.5914	0.4167	0.4878	0.3989	0.4352	1.2840	0.3690	0.6755
Eastern Cottontail	0.4002	0.3786	0.3504	0.6118	0.3854	0.4797	0.3074	1.4792	0.5401	0.8701
European Hare	0.2724	0.3752	0.4786	0.4666	0.2312	0.3403	0.2451	1.3326	0.3462	0.7213
F-15	0.3156	0.4404	0.5435	0.4285	0.4403	0.3422	0.3120	1.2957	0.3216	0.6856
F-16	0.3566	0.4503	0.5601	0.3599	0.3265	0.3194	0.3805	1.0571	0.3442	0.4489
Harrier	0.3226	0.2729	0.3851	0.4913	0.4356	0.3270	0.3071	1.3579	0.3174	0.7468
Mig	0.5094	0.5006	0.3682	0.5323	*0.2853*	0.5226	0.3516	1.3447	0.318	0.7335
Phantom	0.3422	0.5006	0.6731	0.3257	0.4740	0.2846	0.5288	0.9090	0.3621	0.3126
Hand	**0.0189**	0.4170	0.5190	0.2878	0.3439	0.3278	0.3039	1.1481	*0.2333*	0.5360
Hand10	0.4334	**0.0483**	*0.2184*	0.6015	0.2792	0.5115	0.3413	1.1284	0.5712	0.6343
Hand90	0.4987	*0.2193*	**0.0231**	0.6723	0.2755	0.5800	0.2528	1.2614	0.6413	0.7058
Handbent1	*0.2711*	0.5868	0.6945	**0.0293**	0.4984	0.3306	0.5527	0.8848	0.2949	0.2779
Handbent2	0.3468	0.2859	0.3007	0.5143	**0.0271**	0.3109	*0.2242*	1.3813	0.3650	0.7706
Bone Fish	0.3477	0.4985	0.6038	0.3455	0.3213	**0.0382**	0.3301	1.1278	0.2909	0.5166
Cardinal Fish	0.3172	0.3549	0.2741	0.5841	*0.2415*	0.3661	**0.0323**	1.4514	0.3955	0.8427
Dogfish Shark	1.1515	1.1315	1.2632	0.8705	1.3858	1.0928	1.4406	**0.0223**	1.0612	*0.6154*
Goat Fish	*0.2198*	0.5351	0.6415	0.2597	0.3451	0.2750	0.3911	1.0483	**0.0665**	0.4379
Herrings	0.5284	0.6187	0.7270	*0.2943*	0.7643	0.4706	0.8211	0.6200	0.4398	**0.0229**

We now examine a larger set of images from the Kimia silhouette database. We compare 5 different types of rabbits, 5 types of planes, 5 different hands, and 5 different types of fish to small perturbations of each original image. Specifically, as in the small example in Table 4.1, we will compare the signature for an arctic hare with the signature for a small perturbation of the arctic hare. The original image's signature will also be compared with signature curves for small perturbations of the other 19 images. The results are given in Tables 4.2 and 4.3.

Note that as in the small example, the smallest distance occurs when the original image is compared to a small perturbation of that image. These smallest distances are boldfaced. The italicized entries refer to the next smallest distance. We want the distance to be defined such that the next smallest distance will be between the original image and another image from that class. For example, if we look at the arctic hare, we want the next smallest distance to be between the arctic hare and another rabbit. In the tables, we see that this is sometimes the case, but in some of the comparisons it is not. For example, notice that the next smallest distance for the dogfish shark is a small perturbation of the herrings image, but the next smallest distance for the arctic hare is with a small perturbation of the hand. We compare our results with those obtained in [39].

Previous Work In [39], Manay et al. focus on closed curves with no self-intersections and define an area integral invariant. For each point p on the curve γ, they define a ball of radius r centered at p for some chosen value of r. Let $Int(B_r)$ refer to the interior of the ball of radius r centered at p, and let $Int(\gamma)$ refer to the interior of the curve γ. Then the area of $Int(B_r) \cap Int(\gamma)$ is an integral invariant under the Euclidean action

and will be denoted by $\mathcal{A}_\gamma$. For an illustration, see Figure 4.2. In the figure, the curve of interest is denoted by C, and $int(C) = \overline{C}$.

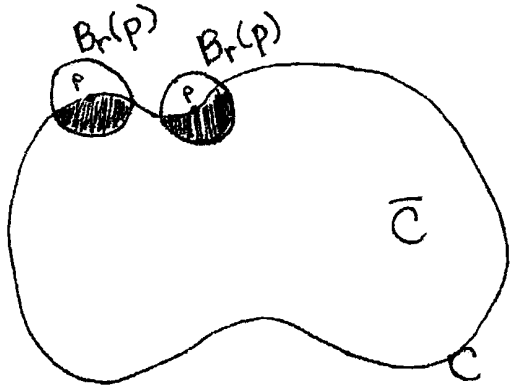

Figure 4.2: Integral invariant $\mathcal{A}_\gamma$ from [39]

Manay et al. remark that a naive approach for distance would be to look at the difference between integral invariants. For this approach to have meaning, one would have to compare similar parts of images. For instance, if the ears of a rabbit were compared to the tail of another rabbit, then the distance between integral invariants may be very large. Thus it is necessary to find the optimal correspondence between points on the two shapes.

To find the optimal correspondence between points, the authors reparametrize the curves and integral invariants by the use of what they call a disparity function. They denote the disparity function by $d(s)$, where s is the arc length parameter. This disparity function accounts for curves with different lengths. Then they define an energy functional based on d and the integral invariants $\mathcal{A}_{\gamma_1}$, $\mathcal{A}_{\gamma_2}$ for curves γ_1 and γ_2.

The energy functional is given by

$$E(\mathcal{A}_{\gamma_1}, \mathcal{A}_{\gamma_2}, d) = \int_0^1 ||\mathcal{A}_{\gamma_1}(s - d(s)) - \mathcal{A}_{\gamma_2}(s + d(s))||^2 ds + \alpha ||d'(s)||^2 ds, \qquad (4.4)$$

where $\alpha > 0$ is a constant. The constant α is a control parameter. The effect of α is illustrated in Figure 4.3, taken from [39]. In the figure, (a) corresponds to $\alpha = 100$, (b) corresponds to $\alpha = 30$, and (c) corresponds to $\alpha = 1$. They observe that smaller values for α emphasize geometrical differences.

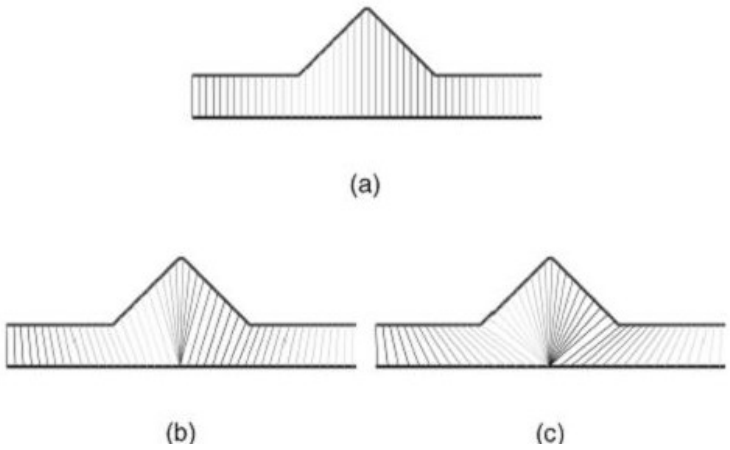

Figure 4.3: Effects of control parameter

The disparity function that minimizes the energy functional in Equation (4.4) is denoted by $d^*(s)$. This function is defined by minimizing 4.4, then interchanging γ_1 and γ_2 and minimizing again. Then $d^*(s)$ is defined as the minimum between the two. Use of $d^*(s)$ ensures that the distance between equivalence classes of curves is symmetric, i.e. neither curve is favored over the other. Then the group invariant distance between

equivalence classes of curves is defined as

$$\mathcal{D}(\gamma_1, \gamma_2) = E(\mathcal{A}_{\gamma_1}, \mathcal{A}_{\gamma_2}, d^*). \tag{4.5}$$

There is still the issue of choosing an initial point and initial correspondence. A quick way of determining the best initial correspondence does not exist. Oftentimes, an exhaustive search is used. In such a search, one chooses a fixed point on one curve and compares it with each point on the other curve to find the shortest path between the two. Manay et al. note that the exhaustive search can be avoided by looking at strong features. For example, corners may be used to find the optimal initial correspondence quickly. The authors use $\mathcal{A}_{\gamma_1}$ for points with little to no curvature to define a subset of points outside the ball used to determine $\mathcal{A}_{\gamma_1}$. Then the set of points outside the ball and their nearest neighbors on $\mathcal{A}_{\gamma_2}$ are likely initial correspondences.

Using the Hausdorff distance between integral signatures to define the distance between congruence classes of curves is much less involved than the method presented in [39]. However, Manay et al. get better results with their method.

Conclusions and Future Work In this thesis, we investigated several different integral invariants and signatures for the action of the Euclidean group on planar curves. In the future we want to improve our methods of curve matching, and investigate integral invariants and signatures for other group actions, such as the affine and projective groups. It would also be of interest to explore the possibility of extending our methods to curves in $\mathbb{R}^3$.

To implement our methods, we used the trapezoid rule to estimate integrals. The

advantage to using trapezoid rule is that the approximation of I_1 is invariant as shown in Chapter 3. The trapezoid rule however is not a very efficient method for approximating integrals. We would like to investigate the use of other methods and note that it is desirable to have a numerical approximation that is group invariant.

To compute local integral invariants and local integral signatures, we partitioned the curve into equal length intervals, Δ_l, for $l = 1, \ldots m$. Our approximations of I_1^{loc} and I_2^{loc} depend on the choice of the number of intervals, m. A more careful study of dependence of the result on the choice of m is needed. When m is small, we do not capture enough of the curve. If we look at a perturbation of a curve and choose a large value of m, we capture a lot of the perturbation.

In addition to investigating the use of various integral signatures for curve matching, we defined a distance between congruence classes of curves. In particular, we defined distance between congruence classes as the Hausdorff distance between signature curves. We focused on the Hausdorff distance between $(\overline{I_1^{loc}}, \overline{I_2^{loc}})$ signatures for shapes from the Kimia silhouette database.

It may be of interest in the future to run distance experiments using the Hausdorff distance on the $(l, I_1^{loc}(l))$ signatures. Recall that the $(l, I_1^{loc}(l))$ signature depends on initial point, but in a predictable way. The change of initial point corresponds to a translation of the signature. The $(l, I_1^{loc}(l))$ signature is of particular interest because the approximation of $I_1^{loc}(l)$ is invariant, using trapezoid rule.

When comparing the Hausdorff distance between signature curves for real images, we found that the smallest distance is between the image and a small perturbation of that image. However, the next smallest distance is not always what we expect.

It may be useful looking at other possible definitions for distance. Recall however that the advantage to Hausdorff distance is that it does not require synchronization of parameters. In choosing a distance function, it is also desirable for the computation to be group invariant.

We would also like to look at the distance between congruence classes of curves under the affine group action. Integral signatures for the affine group action are explored in [23]. Another problem of interest is to match curves under the projective action using integral signatures and Hausdorff distance. There are challenges defining strictly integral invariants for the projective action, so it may be worthwhile to begin with applying Hausdorff distance to integro-differential invariants such as those in [53].

References

[1] Alex Abatzoglou, Mandy Smith, Jessica WebsertLove, Kathleen Iwancio, and Irina Kogan. Invariants in computer vision. Technical report, North Carolina State University, 2007.

[2] Mahmood Akhtar, Eliathamby Ambikairajah, and Julien Epps. Digital signal processing techniques for gene finding in eukaryotes. In *ICISP*, pages 144–152, 2008.

[3] Smaïl Akkoul, Roger Lédée, Remy Leconge, Christophe Léger, Rachid Harba, Sabrina Pesnel, Stéphanie Lerondel, Alain Lepape, and Luis Vilcahuaman. Comparison of image restoration methods for bioluminescence imaging. In *ICISP*, pages 163–172, 2008.

[4] Mohamed A. Ali. Arabic handwritten characters classification using learning vector quantization algorithm. In *ICISP*, pages 463–470, 2008.

[5] Aaron D. Ames, Jeffrey A. Jalkio, and Cheri Shakiban. Three-dimensional object recognition using invariant Euclidean signature curves. In *Analysis, combinatorics and computing*, pages 13–23. Nova Sci. Publ., Hauppauge, NY, 2002.

[6] Aouatif Amine, Mohammed Rziza, and Driss Aboutajdine. Svm-based face recognition using genetic search for frequency-feature subset selection. In *ICISP*, pages 321–328, 2008.

[7] M. Amrouch, M. Elyassa, A. Rachidi, and D. Mammass. Off-line arabic handwritten characters recognition based on a hidden markov models. In *ICISP*, pages 447–454, 2008.

[8] Michael Artin. *Algebra*. Prentice Hall Inc., Englewood Cliffs, NJ, 1991.

[9] Eamon B. Barrett, Michael H. Brill, Nils N. Haag, and Paul M. Payton. Invariant linear methods in photogrammetry and model-matching. In *Geometric invariance*

in computer vision, Artificial Intelligence, pages 277–292. MIT Press, Cambridge, MA, 1992.

[10] Rachid Belaroussi and Guillaume Morel. Combination of image registration algorithms for patient alignement in proton beam therapy. In *ICISP*, pages 183–191, 2008.

[11] P. Bilane, Stéphane Bres, and Hubert Emptoz. Local orientation extraction for wordspotting in syriac manuscripts. In *ICISP*, pages 481–489, 2008.

[12] Michael H. Brill, Eamon B. Barrett, and Paul M. Payton. Projective invariants for curves in two and three dimensions. In *Geometric invariance in computer vision*, Artificial Intelligence, pages 193–214. MIT Press, Cambridge, MA, 1992.

[13] B.G. Burdea and H.J. Wolfson. Solving jigsaw puzzles by a robot. *Robotics and Automation, IEEE Transactions on*, 5(6):752–764, Dec 1989.

[14] Eugenio Calabi, Peter J. Olver, Chehrzad Shakiban, Allen Tannenbaum, and Steven Haker. Differential and numerically invariant signature curves applied to object recognition. *Int. J. Comput. Vision*, 26(2):107–135, 1998.

[15] John Canny. A computational approach to edge detection. *Pattern Analysis and Machine Intelligence, IEEE Transactions on*, PAMI-8(6):679–698, Nov. 1986.

[16] É. Cartan. Groupes finis et continus et la géométrie différentielle traitées par la methode du repère mobile. 1937.

[17] Jingying Chen and Bernard Tiddeman. Multi-cue facial feature detection and tracking. In *ICISP*, pages 356–367, 2008.

[18] Christopher Coelho, Aaron Heller, Joseph L. Mundy, David A. Forsyth, and Andrew Zisserman. An experimental evaluation of projective invariants. In *Geometric invariance in computer vision*, Artificial Intelligence, pages 87–104. MIT Press, Cambridge, MA, 1992.

[19] Harm Derksen and Gregor Kemper. *Computational invariant theory*. Invariant Theory and Algebraic Transformation Groups, I. Springer-Verlag, Berlin, 2002. Encyclopaedia of Mathematical Sciences, 130.

[20] Martin Donnelley, Greg Knowles, and Trevor Hearn. A cad system for long-bone segmentation and fracture detection. In *ICISP*, pages 153–162, 2008.

[21] Tiwuya H. Faaya and Önsen Toygar. Illumination invariant face recognition under various facial expressions and occlusions. In *ICISP*, pages 304–311, 2008.

[22] Mark Fels and Peter J. Olver. Moving frames and coframes. In *Algebraic methods in physics (Montréal, QC, 1997)*, CRM Ser. Math. Phys., pages 47–64. Springer, New York, 2001.

[23] Shuo Feng, Irina Kogan, and Hamid Krim. Classifications of curves in 2D and 3D via affine integral signatures. *To appear in Acta Applicandae Mathematicae.*

[24] David Goldberg, Christopher Malon, and Marshall Bern. A global approach to automatic solution of jigsaw puzzles. *Comput. Geom.*, 28(2-3):165–174, 2004.

[25] Oleg Golubitsky, Vadim Mazalov, and Stephen M. Watt. Orientation-independent recognition of handwritten characters with integral invariants. *Proc. 9th Asian Symposium on Computer Mathematics, (ASCM 2009) (to appear).*

[26] Mark L. Green. The moving frame, differential invariants and rigidity theorems for curves in homogeneous spaces. *Duke Math. J.*, 45(4):735–779, 1978.

[27] P. Griffiths. On Cartan's method of Lie groups and moving frames as applied to uniqueness and existence questions in differential geometry. *Duke Math. J.*, 41:775–814, 1974.

[28] Mohamed El hajji, Hassin Douzi, and Rachid Harba. Watermarking based on the density coefficients of faber-schauder wavelets. In *ICISP*, pages 455–462, 2008.

[29] C. E. Hann and M. S. Hickman. Projective curvature and integral invariants. *Acta Appl. Math.*, 74(2):177–193, 2002.

[30] M.D. Heath, S. Sarkar, T. Sanocki, and K.W. Bowyer. A robust visual method for assessing the relative performance of edge-detection algorithms. *Pattern Analysis and Machine Intelligence, IEEE Transactions on*, 19(12):1338–1359, Dec 1997.

[31] John E. Hopcroft, Daniel P. Huttenlocher, and Peter C. Wayner. Affine invariants for model-based recognition. In *Geometric invariance in computer vision*, Artificial Intelligence, pages 354–374. MIT Press, Cambridge, MA, 1992.

[32] M.K. Hu. Visual pattern recognition by moment invariants. In *IRE Transactions on Information Theory*, pages 179–187, 1962.

[33] D.P. Huttenlocher, G.A. Klanderman, and W.J. Rucklidge. Comparing images using the Hausdorff distance. *Pattern Analysis and Machine Intelligence, IEEE Transactions on*, 15(9):850–863, Sep 1993.

[34] Guillaume Joutel, Véronique Eglin, and Hubert Emptoz. A complete pyramidal geometrical scheme for text based image description and retrieval. In *ICISP*, pages 471–480, 2008.

[35] Deepak Kapur and Joseph L. Mundy. Fitting affine invariant conics to curves. In *Geometric invariance in computer vision*, Artificial Intelligence, pages 252–266. MIT Press, Cambridge, MA, 1992.

[36] Irina A. Kogan. Two algorithms for a moving frame construction. *Canad. J. Math.*, 55(2):266–291, 2003.

[37] Peter D. Kukharchik, Igor E. Kheidorov, Eugeny E. Bovbel, and D. Ladeev. Speech signal processing based on wavelets and svm for vocal tract pathology detection. In *ICISP*, pages 192–199, 2008.

[38] Cheng-Lin Liu, Kazuki Nakashima, Hiroshi Sako, and Hiromichi Fujisawa. Handwritten digit recognition: investigation of normalization and feature extraction techniques. *Pattern Recognition*, 37(2):265 – 279, 2004.

[39] S. Manay, D. Cremers, Byung-Woo Hong, A.J. Yezzi, and S. Soatto. Integral invariants for shape matching. *Pattern Analysis and Machine Intelligence, IEEE Transactions on*, 28(10):1602–1618, Oct. 2006.

[40] S. Manay, Byung-Woo Hong, A.J. Yezzi, and S. Soatto. Integral invariant signatures. *Proc. European Conf. Computer Vision*, May 2004.

[41] D. Marr and E. Hildreth. Theory of edge detection. *Proceedings of the Royal Society of London. Series B, Biological Sciences*, 207(1167):187–217, 1980.

[42] Roger Mohr, Luce Morin, and Enrico Grosso. Relative positioning with uncalibrated cameras. In *Geometric invariance in computer vision*, Artificial Intelligence, pages 440–460. MIT Press, Cambridge, MA, 1992.

[43] R. Mukundan and K.R. Ramakrishnan. *Moment Functions in Image Analysis: Theory and Applications*. World Scientific Publishing Co., 1998.

[44] Joseph L. Mundy and Andrew Zisserman, editors. *Geometric invariance in computer vision*. Artificial Intelligence. MIT Press, Cambridge, MA, 1992.

[45] Mark Nixon and Alberto Aguado. *Feature Extraction & Image Processing*. Newnes.

[46] Peter J. Olver. *Equivalence, invariants, and symmetry*. Cambridge University Press, Cambridge, 1995.

[47] Peter J. Olver. *Classical invariant theory*, volume 44 of *London Mathematical Society Student Texts*. Cambridge University Press, Cambridge, 1999.

[48] Peter J. Olver. Joint invariant signatures. *Foundations of Computational Mathematics*, 1(1):3–68, 2001.

[49] J.R. Parker. *Algorithms for Image Processing and Computer Vision*. John Wiley & Sons, Inc., New York, 1997.

[50] J.M.S. Prewitt and M.L. Mendelsohn. The analysis of cell images. *Ann. N.Y. Acad. Sci.*, pages 1035–1053, 1966.

[51] L.G. Roberts. Machine perception of three-dimensional solids. Optical and Electro-Optical Information Processing, pages 159–197. MIT Press, 1965.

[52] Charles A. Rothwell, Andrew Zisserman, David A. Forsyth, and Joseph L. Mundy. Fast recognition using algebraic invariants. In *Geometric invariance in computer vision*, Artificial Intelligence, pages 398–407. MIT Press, Cambridge, MA, 1992.

[53] Jun Sato and Roberto Cipolla. Affine integral invariants for extracting symmetry axes. *Image and Vision Computing*, 15(8):627–635, 1997.

[54] Daniel Sharvit, Jacky Chan, Huseyin Tek, and Benjamin B. Kimia. Symmetry-based indexing of image databases. *http://www.lems.brown.edu/vision/software/index.html*.

[55] Jun Shen and Serge Castan. An optimal linear operator for step edge detection. *CVGIP: Graphical Models and Image Processing*, 54(2):112 – 133, 1992.

[56] Nicolas Signolle, Benoît Plancoulaine, Paulette Herlin, and Marinette Revenu. Texture-based multiscale segmentation: Application to stromal compartment characterization on ovarian carcinoma virtual slides. In *ICISP*, pages 173–182, 2008.

[57] Elena Smirnova and Stephen M. Watt. Communicating mathematics via pen-based interfaces. In *Tenth International Symposium on Symbolic and Numeric Algorithms for Scientific Computing*, pages 9–18. IEEE Computer Society, 2008.

[58] I.E. Sobel. *Camera Models and Machine Perception*. PhD thesis, Stanford University.

[59] Gabriel Taubin and David B. Cooper. Object recognition based on moment (or algebraic) invariants. In *Geometric invariance in computer vision*, Artificial Intelligence, pages 375–397. MIT Press, Cambridge, MA, 1992.

[60] Luc J. Van Gool, Theo Moons, Eric Pauwels, and André Oosterlinck. Semi-differential invariants. In *Geometric invariance in computer vision*, Artificial Intelligence, pages 157–192. MIT Press, Cambridge, MA, 1992.

[61] È. B. Vinberg and V. L. Popov. Invariant theory. In *Algebraic geometry, 4 (Russian)*, Itogi Nauki i Tekhniki, pages 137–314, 315. Akad. Nauk SSSR Vsesoyuz. Inst. Nauchn. i Tekhn. Inform., Moscow, 1989.

[62] Isaac Weiss. Noise resistant invariants of curves. In *Geometric invariance in computer vision*, Artificial Intelligence, pages 135–156. MIT Press, Cambridge, MA, 1992.

[63] Haim Wolfson, Edith Schonberg, Alan Kalvin, and Yehezkel Lamdan. Solving jigsaw puzzles by computer. *Ann. Oper. Res.*, 12(1-4):51–64, 1988.

[64] H.J. Wolfson. On curve matching. *Pattern Analysis and Machine Intelligence, IEEE Transactions on*, 12(5):483–489, May 1990.

[65] D. Xu and H. Li. 3-d affine moment invariants generated by geometric primitives. In *Proceedings of ICPR*, pages 544–547, 2006.

[66] Chunjiang Zhao, Wenkang Shi, and Yong Deng. A new Hausdorff distance for image matching. *Pattern Recognition Letters*, 26(5):581 – 586, 2005.

[67] Andrew Zisserman, David A. Forsyth, Joseph L. Mundy, and Charles A. Rothwell. Recognizing general curved objects efficiently. In *Geometric invariance in computer vision*, Artificial Intelligence, pages 228–251. MIT Press, Cambridge, MA, 1992.

[68] Nello Zuech. *Applying Machine Vision*. John Wiley & Sons, Inc., New York, 1988.